Electronic supplementary information

Isomeric Modulation of Thermally Activated Delayed Fluorescence in Dibenzo[a,c]phenazine-based (Deep) Red Emitters

Sonny Brebels[a,b,c], Tom Cardeynaels[a,b,c,d], Louis Jackers[a,b,c], Suman Kuila[e], Huguette Penxten[a,b,c], Rebecca J. Salthouse[f], Andrew Danos*[e], Andrew P. Monkman[e], Benoît Champagne[d], and Wouter Maes*[a,b,c]

[a] Hasselt University, Institute for Materials Research (IMO-IMOMEC), Design & Synthesis of Organic Semiconductors (DSOS), Agoralaan 1, 3590 Diepenbeek, Belgium; E-mail: wouter.maes@uhasselt.be
[b] IMOMEC Division, IMEC, Wetenschapspark 1, 3590 Diepenbeek, Belgium
[c] Energyville, Thorpark, 3600 Genk, Belgium
[d] University of Namur, Laboratory of Theoretical Chemistry, Theoretical and Structural Physical Chemistry Unit, Namur Institute of Structured Matter, Rue de Bruxelles 61, 5000 Namur, Belgium
[e] Durham University, Department of Physics, OEM group, South Road, Durham DH1 3LE, United Kingdom;
E-mail: andrew.danos@durham.ac.uk
[f] Durham University, Department of Chemistry, South Road, Durham DH1 3LE, United Kingdom

Table of contents

1. Materials and methods

All commercially available reagents were obtained from Acros Organics, Alfa Aesar, BLD Pharmatech, Fluorochem, J&K Scientific, Sigma-Aldrich, STREM Chemicals, TCI Europe, or VWR Chemicals and were used without further purification. Solvents were obtained from Fisher Scientific, Sigma-Aldrich, or VWR Chemicals and were used without further purification. Dry solvents were obtained from an MBraun solvent purification system (MB SPS-800) equipped with alumina columns. Preparative (recycling) size exclusion chromatography (SEC) was performed on a JAI LC-9110 NEXT system equipped with JAIGEL 1H and 2H columns (eluent chloroform, flow rate 3.5 mL min^{-1}) or a JAI LaboACE LC-7080 Plus with with JAIGEL 1H and 2H columns (eluent chloroform, flow rate 10 mL min^{-1}). Proton and carbon nuclear magnetic resonance (^{1}H and ^{13}C NMR) spectra were obtained on a Jeol spectrometer operating at 400 MHz for ^{1}H (100 MHz for ^{13}C). Chemical shifts (δ) are given in ppm relative to $CDCl_3$ (δ = 7.26 ppm for ^{1}H NMR, δ = 77.16 ppm for ^{13}C NMR) or DMSO-d_6 (δ = 2.50 ppm for ^{1}H NMR, δ = 39.52 ppm for ^{13}C NMR). Coupling constants are given in Hz. Matrix-assisted laser desorption/ionization - time-of-flight (MALDI-ToF) mass spectra were recorded on a Bruker Daltonics UltrafleXtreme MALDI/ToF-ToF system. 10 µL of the matrix solution consisting of 20 mg/mL trans-2-[3-(4-tert-butylphenyl)-2-methyl-2-propenylidene]malononitrile (DTCB) in chloroform was mixed with 3.5 µL analyte solution of approximately 1 mg/mL in chloroform. Then, 1 µL of said mixed solution was spotted onto an MTP Anchorchip 600/384 MALDI plate. Purification of the final products was performed by vacuum sublimation using a DSU-05/20 tube-based vacuum sublimation setup from CreaPhys GmbH. The source materials were evaporated at a temperature between 260 and 280 °C and a maximum vacuum pressure of 10^{-6} mbar.

Electronic absorption spectra of the small molecule chromophores in solution were recorded on a Varian Cary 5000 UV-Vis-NIR spectrophotometer from Agilent Technologies. Corrected steady-state excitation and emission spectra in solution were recorded on an Edinburgh FLS100 spectrofluorometer equipped with a 450 W Xe lamp as the light source, with an excitation wavelength (λ_{exc}) depending on the fluorescence quantum yield standard used. Corrected steady-state excitation and emission spectra of thin films were recorded on a Horiba-Jobin Yvon Fluorolog-3 spectrofluorometer equipped with a 450 W Xe lamp as the light source, with an excitation wavelength depending on the fluorescence quantum yield standard used. Freshly prepared samples in 1 cm quartz cells were used to perform all UV-Vis-NIR absorption and fluorescence measurements. The fluorescence measurements were done under a right-angle arrangement. The standard uncertainty (square root of the variance) on the absorption and emission maxima is approximately 1 nm. Spectroscopic measurements under normal atmosphere were done in non-degassed spectroscopic grade solvents at 20 °C. Inert atmosphere was created by three consecutive freeze-pump-thaw cycles.

For the determination of the relative fluorescence quantum yields (Φ_F) in toluene, dilute solutions with an absorbance around 0.1 at the excitation wavelength were used. Coumarin 153 (λ_{exc} = 440 nm, Φ_F = 0.38 in ethanol) was used as a standard to determine the fluorescence quantum yields.[1] The fluorescence quantum yield of the tested compound (Φ_x) was calculated using **Equation S1**, in which Φ_{st} is the fluorescence quantum yield of the standard, F_x and F_{st} are the integrated fluorescence of the test compound and the standard, A_x and A_{st} are the absorbance of the test compound and the standard at the excitation wavelength, and n_x and n_{st} are the refractive indices of the solvents in which the test compound and the standard were dissolved, respectively.

$$\Phi_x = \Phi_{st}\frac{F_x\left(1-10^{-A_{st}}\right)n_x{}^2}{F_{st}\left(1-10^{-A_x}\right)n_{st}{}^2} \quad (\mathbf{S1})$$

1,3-Diphenylisobenzofuran (1,3-DPBF) was used as a singlet oxygen ($^1O_2$) scavenger to determine the singlet oxygen quantum yields (Φ_Δ). The $^1O_2$ production was monitored by following the absorbance of 1,3-DPBF at 414 nm upon excitation of the respective chromophore at 325 nm using a single LED325W2 from Thorlabs (λ_{exc} = 325±5 nm, fwhm = 11 nm, P = 1.7 mW). To determine Φ_Δ, a relative method was used according to **Equation S2**. Here, '*x*' and '*st*' represent the sample and the standard, while Φ, *A*, *m*, and *n* represent the singlet oxygen quantum yield, the absorbance at the excitation wavelength (λ_{exc} = 325 nm), the slope of the decrease in absorbance of 1,3-DPBF over time, and the refractive index of the solvent used for the measurement, respectively. Optically matched solutions with an absorbance around 0.6 at 414 nm and 0.3 at 325 nm were used. Coronene was used as the standard (Φ_Δ = 0.90 in spectrograde toluene).[2] The solutions were continuously stirred during all measurements using a Cimarec magnetic stirrer.

$$\Phi_x = \Phi_{st}\left(\frac{1-10^{-A_{st}}}{1-10^{-A_x}}\right)\left(\frac{m_x}{m_{st}}\right)\left(\frac{n_x}{n_{st}}\right)^2 \quad (\mathbf{S2})$$

Zeonex films were prepared via drop-casting using a mixture of the emitter and host (zeonex) in toluene at 0.1 wt%. The initial solution concentrations consisted of 100 mg mL^{-1} of zeonex and 0.1 mg mL^{-1} of emissive material. Bis[2-(diphenylphosphino)phenyl]ether oxide (DPEPO) and 4,4′-bis(*N*-carbazolyl)-1,1′-biphenyl (CBP) films were prepared via drop-casting using a mixture of the emitter and host (DPEPO or CBP) in toluene at 1 wt%. The initial solution concentrations consisted of 1 mg mL^{-1} of CBP or DPEPO and 0.1 mg mL^{-1} of emissive material. The films were drop-casted onto a quartz substrate at 65 °C to facilitate evaporation of the solvent. Time-resolved photoluminescence spectra and decays of the thin film samples were recorded using a nanosecond gated spectrograph-coupled iCCD (Stanford) using an Nd:YAG laser emitting at 355 nm (EKSPLA) under vacuum. Photoluminescence quantum yields in film were determined using a calibrated integrating sphere (Horiba Quanta-Phi) fibre-coupled to a spectrofluorometer (Horiba Fluorolog) as excitation source (450 nm) and detection system. For the measurements in inert atmosphere, the sphere was flushed with a stream of dry nitrogen for at least 30 min to prevent oxygen quenching of triplets.

Cyclic voltammetry (CV) was carried out in argon-purged acetonitrile at room temperature with an Autolab potentiostat (PGSTAT30 from Metrohm) controlled with GPES software (version 4.9) for data collection and analysis. Tetrabutylammonium hexafluorophosphate ($TBAPF_6$) (0.1 M) was used as the supporting electrolyte. A one-compartment microcell designed for three-electrode configuration was fitted with a platinum wire working electrode, a platinum wire counter electrode, and an $Ag/AgNO_3$ reference electrode (Ag wire immersed in electrolyte containing 0.01 M $AgNO_3$). A film of the analyte was deposited on the working electrode by casting it from a chlorobenzene solution. Voltammograms were recorded at a scan rate of 100 mV s^{-1} under a constant flow of argon, allowing degassing and blanketing of the electrolyte before and during analysis. Typically, 5 scans per film were recorded and HOMO/LUMO energy levels were estimated from the averaged onset potentials of the 3rd, 4th, and 5th scan. In this particular case, HOMO/LUMO energy levels were also estimated from the onset potentials of the 1st scan to account for dimer formation in subsequent scans. The onset potential was determined from the intersection of two tangents drawn at the rising and background current of the cyclic voltammogram. Ferrocene was used as an external standard. For the conversion of potentials (in V) obtained from the electrochemical measurements to frontier molecular orbital energies (in eV), the formal potential of the Fc/Fc^+ redox couple was scaled to the vacuum level with a value of –4.98 eV, considering that 0.0 V on the ferrocene scale corresponds to 0.31 V versus SCE (0.55 V versus SHE) and that 0.0 V versus SHE is equivalent to –4.44 eV (**Equation S3**).[3, 4]

$$\text{HOMO/LUMO (eV)} = -4.98\ \text{(eV)} - E_{onset}\ \text{(analyte) vs } Ag/AgNO_3\ \text{(V)} + E_f\ (Fc/Fc^+)\ \text{vs } Ag/AgNO_3\ \text{(V)} \quad \textbf{(S3)}$$

The X-ray single crystal data for **3-TPA-DBPzCN** have been collected at a temperature of 120.0(2)K using MoKα radiation (λ =0.71073Å) on a Bruker D8Venture (Photon III MM C14 CPAD detector, IμS-III-microsource, focusing mirrors) 3-circle diffractometer equipped with a Cryostream (Oxford Cryosystems) open-flow nitrogen cryostat. The structure was solved by direct method and refined by full-matrix least squares on F2 for all data using Olex2[5] and SHELXTL[6] software. All non-hydrogen atoms were refined in anisotropic approximation, while hydrogen atoms were located in the difference Fourier map and refined isotropically. Crystal data and parameters of refinement are listed in Table S6. Crystallographic data for the structure has been deposited with the Cambridge Crystallographic Data Centre as supplementary publication CCDC-2354499.

2. Materials synthesis

1-Bromophenanthrene (**1-1**) and 4-bromophenanthrene (**1-4**) were synthesized according to literature procedures.[7, 8]

*1-bromophenanthrene-9,10-dione (**2-1**)*

General procedure 1: 1-Bromophenanthrene (514 mg, 2 mmol) and chromium(VI) oxide (700 mg, 7 mmol) were added to a flame-dried round bottom flask and dissolved in glacial acetic acid (35 mL). The flask was preheated to ensure all material was properly dissolved. Next, the reaction mixture was stirred and heated to reflux for two hours. After cooling down to room temperature, the mixture was poured into water (50 mL), vacuum filtered, and washed multiple times with water. After drying, 1-bromophenanthrene-9,10-dione was obtained as an orange solid (346 mg, 60%). 1H NMR (400 MHz, DMSO-d_6) δ 8.30 (d, J = 7.9 Hz, 1H), 8.25 (d, J = 8.1 Hz, 1H), 8.01 (d, J = 7.7 Hz, 1H), 7.87 – 7.68 (m, 2H), 7.68 – 7.44 (m, 2H). ^{13}C NMR (100 MHz, DMSO-d_6) δ 180.4, 180.1, 139.0, 136.6, 136.4, 135.9, 135.7, 131.1, 130.4, 129.6, 129.3, 125.8, 125.4, 124.3.

*4-bromophenanthrene-9,10-dione (**2-4**)*

Synthesis according to general procedure 1: 4-bromophenanthrene (771 mg, 3 mmol), chromium(VI) oxide (1.05 g, 10.5 mmol), glacial acetic acid (50 mL); orange solid (602 mg, 70%). ^{1}H NMR (400 MHz, DMSO-d_6) δ 8.83 (dd, *J* = 8.1, 0.7 Hz, 1H), 8.11 (dd, *J* = 8.0, 1.5 Hz, 1H), 8.06 – 8.00 (m, 2H), 7.86 – 7.80 (m, 1H), 7.60 (td, *J* = 7.5, 1.1 Hz, 1H), 7.44 (t, *J* = 7.8 Hz, 1H). ^{13}C NMR (100 MHz, DMSO-d_6) δ 180.06, 180.05, 142.6, 135.5, 135.2, 134.9, 134.2, 132.1, 130.6, 130.3, 129.6, 129.3, 129.2, 120.2.

*1-(4-(diphenylamino)phenyl)phenanthrene-9,10-dione (**3-1**)*

General procedure 2: To a stirred mixture of 1-bromophenanthrene-9,10-dione (0.15 g, 0.52 mmol), 4-(diphenylamino)-phenylboronic acid (0.17 g, 0.59 mmol), and $Pd(PPh_3)_4$ (0.030 g, 0.026 mmol) in dry toluene (4.5 mL), an aqueous Na_2CO_3 solution (2.0 M, 2.3 mL) was added under argon. The mixture was refluxed for 24 h. After cooling to room temperature, the reaction mixture was poured into water. After extracting with chloroform, drying over anhydrous Na_2SO_4 and filtration of the drying agent, the solvent was removed under reduced pressure. The crude product was purified by column chromatography on silica gel (eluent: petroleum ether/dichloromethane = 3:7, v/v) to give **3-1** as a black solid (164 mg, 70%). ^{1}H NMR (400 MHz, Chloroform-*d*) δ 8.14 (dd, *J* = 7.8, 1.5 Hz, 1H), 8.06 (d, *J* = 8.1 Hz, 1H), 8.02 (dd, *J* = 8.2, 0.9 Hz, 2H), 7.77 – 7.70 (m, 1H), 7.67 (t, *J* = 7.8 Hz, 1H), 7.47 (td, *J* = 7.5, 1.0 Hz, 1H), 7.33 (dd, *J* = 7.6, 1.1 Hz, 1H), 7.34 – 7.23 (m, 4H), 7.22 – 7.11 (m, 6H), 7.11 – 7.00 (m, 4H). ^{13}C NMR (100 MHz, Chloroform-*d*) δ 183.2, 182.6, 147.8, 147.3, 147.3, 137.3, 136.8, 136.1, 134.9, 134.6, 133.3, 130.9, 130.0, 129.6, 129.4, 129.3, 129.2, 124.72, 124.66, 123.6, 123.2, 123.1. MALDI-ToF MS (*m*/*z*): Calcd. for $C_{32}H_{21}NO_2$ $[M+H]^+$: *m*/*z* 452.17 (100%), found: 452.36.

*2-(4-(diphenylamino)phenyl)phenanthrene-9,10-dione (**3-2**)*

Synthesis according to general procedure 2: 2-bromophenanthrene-9,10-dione (0.20 g, 0.70 mmol), (diphenylamino)-phenylboronic acid (0.22 g, 0.78 mmol), $Pd(PPh_3)_4$ (0.040 g, 0.035 mmol), dry toluene (6 mL), aqueous Na_2CO_3 solution (2.0 M, 3 mL), eluent petroleum ether/dichloromethane (v/v = 3:7); black solid (219 mg, 69%). ^{1}H NMR (400 MHz, Chloroform-*d*) δ 8.39 (d, *J* = 2.1 Hz, 1H), 8.19 (dd, *J* = 7.8, 1.5 Hz, 1H), 8.04 (d, *J* = 8.5 Hz, 1H), 8.02 (d, *J* = 8.0 Hz, 1H), 7.91 (dd, *J* = 8.3, 2.2 Hz, 1H), 7.76 – 7.67 (m, 1H), 7.55 (d, *J* = 8.7 Hz, 2H), 7.46 (td, *J* = 7.5, 1.0 Hz, 1H), 7.33 – 7.27 (m, 4H), 7.18 – 7.12 (m, 6H), 7.10 – 7.03 (m, 2H). ^{13}C NMR (100 MHz, Chloroform-*d*) δ 180.53, 180.48, 148.5, 147.4, 141.9, 136.2, 136.0, 134.0, 133.6, 131.8, 131.4, 130.9, 130.7, 129.5, 129.4, 128.1, 127.6, 125.0, 124.7, 124.0, 123.6, 123.3. MALDI-ToF MS (*m*/*z*): Calcd. for $C_{32}H_{21}NO_2$ $[M+H]^+$: *m*/*z* 452.17 (100%), found: 452.34.

*3-(4-(diphenylamino)phenyl)phenanthrene-9,10-dione (**3-3**)*

Synthesis according to general procedure 2: 3-bromophenanthrene-9,10-dione (1.00 g, 3.5 mmol), 4-(diphenylamino)phenylboronic acid (1.13 g, 3.9 mmol), $Pd(PPh_3)_4$ (0.20 g, 0.175 mmol), dry toluene (30 mL), aqueous Na_2CO_3 solution (2.0 M, 15 mL), eluent petroleum ether/dichloromethane (v/v = 5:5 to 3:7); red solid (1.41 g, 89%). ^{1}H NMR (400 MHz, Chloroform-*d*) δ 8.21 (d, *J* = 8.3 Hz, 1H), 8.20 – 8.17 (m, 1H), 8.16 (d, *J* = 1.7 Hz, 1H), 8.09 (d, *J* = 8.0 Hz, 1H), 7.75 – 7.67 (m, 1H), 7.63 (dd, *J* = 8.2, 1.6 Hz, 1H), 7.57 (d, *J* = 8.7 Hz, 1H), 7.47 (td, *J* = 7.6, 1.0 Hz, 1H), 7.36 – 7.28 (m, 4H), 7.21 – 7.14 (m, 6H), 7.14 – 7.07 (m, 2H). ^{13}C NMR (100 MHz, Chloroform-*d*) δ 180.7, 179.8, 149.1, 148.3, 147.2, 136.3, 135.97, 135.96, 132.3, 131.4, 131.3, 130.6, 129.7, 129.6, 129.3, 128.1, 127.5, 125.2, 124.0, 123.9, 122.9, 121.9. MALDI-ToF MS (*m*/*z*): Calcd. for $C_{32}H_{21}NO_2$ $[M]^+$: *m*/*z* 451.16 (100%), found: 451.21.

*4(4-(diphenylamino)phenyl)phenanthrene-9,10-dione (**3-4**)*

Synthesis according to general procedure 2: 4-bromophenanthrene-9,10-dione (0.144 g, 0.5 mmol), 4-(diphenylamino)-phenylboronic acid (0.223 g, 0.6 mmol), $Pd(PPh_3)_4$ (0.029 g, 0.025 mmol), dry toluene (5 mL), aqueous Na_2CO_3 solution (2.0 M, 2.5 mL), eluent petroleum ether/dichloromethane (v/v = 5/5); black solid (0.120 g, 88%). ^{1}H NMR (400 MHz, Chloroform-*d*) δ 8.15 (dd, *J* = 7.7, 1.6 Hz, 1H), 8.09 – 8.02 (m, 1H), 7.64 (dd, *J* = 7.6, 1.6 Hz, 1H), 7.47 (t, *J* = 7.7 Hz, 1H), 7.37 – 7.27 (m, 6H), 7.25 – 7.21 (m, 1H), 7.19 – 7.13 (m, 6H), 7.13 – 7.03 (m, 4H). ^{13}C NMR (100 MHz, Chloroform-*d*) δ 177.81, 177.75, 143.1, 142.7, 136.7, 134.9, 132.2, 130.5, 130.0, 129.6, 127.0, 126.8, 126.1, 125.3, 125.1, 124.8, 124.5, 124.1, 124.0, 120.1, 118.9, 118.8. MALDI-ToF MS (*m*/*z*): Calcd. for $C_{32}H_{21}NO_2$ $[M]^+$: *m*/*z* 451.16 (100%), found: 451.20.

*1-bromodibenzo[a,c]phenazine-11,12-dicarbonitrile (**4-1**)*

General procedure 3: Glacial acetic acid (3 mL) was purged with N_2 for 30 min. 1-Bromophenanthrene-9,10-dione (144 mg, 0.5 mmol) and 4,5-diaminophthalonitrile (79 mg, 0.5 mmol) were added and the suspension was stirred and heated at reflux for 24 h.

After cooling to room temperature, the mixture was poured into water (30 mL) and then filtered. The precipitate was washed with water and methanol several times, yielding **4-1** as a yellow solid (180 mg, 93%), which was used as such in the subsequent reaction. ^{1}H NMR (400 MHz, DMSO-d_6) δ 9.20 (dd, *J* = 8.0, 1.5 Hz, 1H), 9.08 (s, 1H), 9.06 (s, 1H), 8.87 (d, *J* = 8.2 Hz, 1H), 8.77 (d, *J* = 8.2 Hz, 1H), 8.15 (dd, *J* = 7.8, 1.1 Hz, 1H), 7.94 (ddd, *J* = 8.3, 7.1, 1.5 Hz, 1H), 7.85 (t, *J* = 7.5 Hz, 1H), 7.76 (t, *J* = 8.0 Hz, 1H). No ^{13}C NMR or MALDI-ToF MS spectrum could be obtained due to the poor solubility of this compound.

*2-bromodibenzo[a,c]phenazine-11,12-dicarbonitrile (**4-2**)*

Synthesis according to general procedure 3: glacial acetic acid (3 mL), 2-bromophenanthrene-9,10-dione (172 mg, 0.6 mmol), 4,5-diaminophthalonitrile (95 mg, 0.6 mmol); yellow solid (225 mg, 92%). No ^{1}H NMR, ^{13}C NMR, or MALDI-ToF MS spectrum could be obtained due to the poor solubility of this compound.

*3-bromodibenzo[a,c]phenazine-11,12-dicarbonitrile (**4-3**)*

Synthesis according to general procedure 3: glacial acetic acid (3 mL), 3-bromophenanthrene-9,10-dione (172 mg, 0.6 mmol), 4,5-diaminophthalonitrile (95 mg, 0.6 mmol); yellow solid (216 mg, 88%). No ^{1}H NMR, ^{13}C NMR, or MALDI-ToF MS spectrum could be obtained due to the poor solubility of this compound.

*1-(4-(diphenylamino)phenyl)dibenzo[a,c]phenazine-11,12-dicarbonitrile (**5-1**)*

General procedure 4 (pathway A in Scheme 1): A mixture of 1-(4-(diphenylamino)phenyl)phenanthrene-9,10-dione (100 mg, 0.2 mmol), 4,5-diaminophthalonitrile (40 mg, 0.24 mmol), and hydrochloric acid (37%, 0.1 mL) in EtOH/THF (1:1, v/v mixture; 7 mL) was stirred for 24 h at 40 °C. After cooling to room temperature, the reaction mixture was poured into water. After extracting with dichloromethane, drying over anhydrous Na_2SO_4 and filtration of the drying agent, the solvent was removed under reduced pressure. The crude product was purified by column chromatography on silica gel (eluent: petroleum ether/dichloromethane = 3:7, v/v), but no desired product was isolated.

Altered procedure 4b: Similar to general procedure 4, with a reaction time of 48 h. No desired product was isolated.

Altered procedure 4c: A mixture of 1-(4-(diphenylamino)phenyl)phenanthrene-9,10-dione (100 mg, 0.2 mmol), 4,5-diaminophthalonitrile (40 mg, 0.24 mmol), and glacial acetic acid (7 mL) was stirred for 72 h at reflux temperature. After cooling to room temperature, the reaction mixture was poured into water. After extracting with dichloromethane, drying over anhydrous Na_2SO_4 and filtration of the drying agent, the solvent was removed under reduced pressure. The crude product was purified by column chromatography on silica gel (eluent: petroleum ether/dichloromethane = 3:7, v/v), but no desired product was isolated.

OR

General procedure 5 (pathway B in Scheme 1): To a stirred mixture of 1-bromodibenzo[*a*,*c*]phenazine-11,12-dicarbonitrile **4-1** (123 mg, 0.3 mmol), 4-(diphenylamino)phenylboronic acid (104 mg, 0.36 mmol), and $Pd(PPh_3)_4$ (35 mg, 0.03 mmol) in dry toluene (7.2 mL), an aqueous Na_2CO_3 solution (1.0 M, 2.4 mL) was added under argon. The mixture was refluxed for 24 h. After cooling to room temperature, the reaction mixture was poured into water. After extracting with dichloromethane, drying over anhydrous Na_2SO_4, and filtration of the drying agent, the solvent was removed under reduced pressure. The crude product was purified by column chromatography on silica gel (eluent: petroleum ether/dichloromethane = 5:5 to 1:9, v/v) to give **5-1** as a black solid (50 mg, 31%). This compound was further purified by temperature-gradient sublimation under vacuum. ^{1}H NMR (400 MHz, Chloroform-*d*) δ 9.33 (d, *J* = 7.6 Hz, 1H), 8.72 (s, 1H), 8.63 (s, 1H), 8.61 (s, 1H), 8.01 (s, 1H), 7.96 – 7.74 (m, 3H), 7.67 (dd, *J* = 7.4, 1.1 Hz, 1H), 7.44 – 7.30 (m, 4H), 7.26 – 7.11 (m, 8H), 7.07 (t, *J* = 7.0 Hz, 2H). No ^{13}C NMR spectrum could be obtained due to the poor solubility of this compound. MALDI-ToF MS (*m*/*z*): Calcd. for $C_{40}H_{23}N_5$ $[M]^+$: *m*/*z* 573.20 (100%), found: 573.44.

*2-(4-(diphenylamino)phenyl)dibenzo[a,c]phenazine-11,12-dicarbonitrile (**5-2**)*

Synthesis according to general procedure 4: 2-(4-(diphenylamino)phenyl)phenanthrene-9,10-dione (100 mg, 0.2), 4,5-diaminophthalonitrile (40mg, 0.24 mmol), hydrochloric acid (37%, 0.1 mL), EtOH/THF (v/v = 1/1, 7 mL), eluent petroleum ether/dichloromethane (v/v = 3:7); dark red solid (215 mg, 95%).

OR

Synthesis according to general procedure 5: 2-bromodibenzo[*a*,*c*]phenazine-11,12-dicarbonitrile **4-2** (123 mg, 0.3 mmol), 4-(diphenylamino)phenylboronic acid (104 mg, 0.36 mmol), $Pd(PPh_3)_4$ (35 mg, 0.03 mmol), dry toluene (7.2 mL), aqueous Na_2CO_3 solution (1.0 M, 2.4 mL), eluent petroleum ether/dichloromethane (v/v = 4:6 to 1:9); dark red solid (136 mg, 84%). This compound

was further purified by temperature-gradient sublimation under vacuum. ^{1}H NMR (400 MHz, Chloroform-*d*) δ 9.49 (d, *J* = 2.0 Hz, 1H), 9.30 (dd, *J* = 7.9, 1.4 Hz, 1H), 8.76 (s, 1H), 8.74 (s, 1H), 8.58 (d, *J* = 8.9 Hz, 1H), 8.56 (d, *J* = 8.5 Hz, 1H), 8.10 (dt, *J* = 8.4, 2.2 Hz, 1H), 7.90 (ddd, *J* = 8.2, 7.1, 1.5 Hz, 1H), 7.78 (d, *J* = 7.2 Hz, 1H), 7.74 (d, *J* = 8.6 Hz, 2H), 7.35 – 7.28 (m, 5H), 7.25 – 7.16 (m, 5H), 7.13 – 7.04 (m, 2H). No ^{13}C NMR spectrum could be obtained due to the poor solubility of this compound. MALDI-ToF MS (*m*/*z*): Calcd. for $C_{40}H_{23}N_5$ [M]$^+$: *m*/*z* 573.20 (100%), found: 573.20.

*3-(4-(diphenylamino)phenyl)dibenzo[a,c]phenazine-11,12-dicarbonitrile (**5-3**)*

Synthesis according to general procedure 4: 3-(4-(diphenylamino)phenyl)phenanthrene-9,10-dione (200 mg, 0.4 mmol), 4,5-diaminophthalonitrile (80 mg, 0.48 mmol), hydrochloric acid (37%, 0.2 mL), EtOH/THF (v/v = 1/1; 14 mL), eluent petroleum ether/dichloromethane (v/v = 5:5 to 1:9); red solid (223 mg, 97%).

OR

Synthesis according to general procedure 5: 3-bromodibenzo[*a*,*c*]phenazine-11,12-dicarbonitrile **4-3** (123 mg, 0.3 mmol), 4-(diphenylamino)phenylboronic acid (104 mg, 0.36 mmol), $Pd(PPh_3)_4$ (35 mg, 0.03 mmol), dry toluene (7.2 mL), aqueous Na_2CO_3 solution (1.0 M, 2.4 mL), eluent petroleum ether/dichloromethane (v/v = 4:6 to 1:9); red solid (175 mg, 86%). This compound was further purified by temperature-gradient sublimation under vacuum. ^{1}H NMR (400 MHz, Chloroform-*d*) δ 9.38 (s, 1H), 9.36 (s, 1H), 8.81 (d, *J* = 0.8 Hz, 2H), 8.74 (d, *J* = 1.5 Hz, 1H), 8.67 (d, *J* = 8.2 Hz, 1H), 8.00 (dd, *J* = 8.4, 1.7 Hz, 1H), 7.92 (td, *J* = 7.7, 1.3 Hz, 1H), 7.82 (t, *J* = 7.6 Hz, 1H), 7.71 (d, *J* = 8.6 Hz, 2H), 7.37 – 7.29 (m, 4H), 7.24 – 7.15 (m, 5H), 7.10 (t, *J* = 7.3 Hz, 2H). No ^{13}C NMR spectrum could be obtained due to the poor solubility of this compound. MALDI-ToF MS (*m*/*z*): Calcd. for $C_{40}H_{23}N_5$ [M]$^+$: *m*/*z* 573.20 (100%), found: 573.26.

*4-(4-(diphenylamino)phenyl)dibenzo[a,c]phenazine-11,12-dicarbonitrile (**5-4**)*

Synthesis according to general procedure 4: 4(4-(diphenylamino)phenyl)phenanthrene-9,10-dione (120 mg, 0.26 mmol), 4,5-diaminophthalonitrile (50 mg, 0.34 mmol), hydrochloric acid (37%, 0.15 mL), EtOH/THF (v/v = 1/1; 8 mL), eluent petroleum ether/dichloromethane (v/v = 3:7), black solid (120 mg, 80%). This compound was further purified by temperature-gradient sublimation under vacuum. ^{1}H NMR (400 MHz, Chloroform-*d*) δ 9.36 (m, 1H), 9.25 (dd, *J* = 8.1, 1.2 Hz, 1H), 8.77 (d, *J* = 0.6 Hz, 1H), 8.76 (d, *J* = 0.6 Hz, 1H), 7.83 (dd, *J* = 8.5, 0.7 Hz, 1H), 7.80 – 7.74 (m, 2H), 7.63 (ddd, *J* = 8.1, 7.1, 1.1 Hz, 1H), 7.43 (ddd, *J* = 8.5, 7.1, 1.6 Hz, 1H), 7.37 – 7.23 (m, 6H), 7.23 – 7.14 (m, 6H), 7.10 – 7.04 (m, 2H). No ^{13}C NMR spectrum could be obtained due to the poor solubility of this compound. MALDI-ToF MS (*m*/*z*): Calcd. for $C_{40}H_{23}N_5$ [M]$^+$: *m*/*z* 573.20 (100%), found: 573.23.

3. TDDFT calculations

Table S1. Nature of the various transitions (H = HOMO, L = LUMO), charge-transfer distance (d_{CT}), and change in dipole moment ($\Delta\mu$, excited state dipole – ground state dipole) accompanying the $S_0 \rightarrow S_x$ and $S_0 \rightarrow T_x$ (x = 1,2) transitions in cyclohexane, as determined with TDDFT-TDA and a modified LC-BLYP (ω = 0.17 bohr^{-1}) exchange correlation functional.

Compound	$S_0 \rightarrow S_1$			$S_0 \rightarrow S_2$			$S_0 \rightarrow T_1$			$S_0 \rightarrow T_2$		
	Nature	d_{CT} (Å)[a]	Δμ (D)[b]	Nature	d_{CT} (Å)[a]	Δμ (D)[b]	Nature	d_{CT} (Å)[a]	Δμ (D)[b]	Nature	d_{CT} (Å)[a]	Δμ (D)[b]
DBPzCN	H-2 → L	0.48	1.60	H → L	2.96	10.66	H-2 → L	0.25	0.81	H → L	1.24	2.42
1-TPA-DBPzCN	H → L (82%)	3.37	18.93	H-1 → L (17%) H-2 → L (15%) H-3 → L (15%) H-9 → L (14%) H → L (12%)	1.84	7.13	H → L (60%) H-1 → L (15%)	2.85	13.33	H-3 → L (29%) H → L (23%) H-2 → L (19%) H-9 → L (13%)	2.08	7.13
2-TPA-DBPzCN	H → L (70%)	5.01	23.89	H-6 → L (59%) H-5 → L (34%)	0.49	1.63	H-1 → L (42%) H → L (37%)	3.75	12.31	H-6 → L (52%) H-5 → L (36%)	0.25	0.82
3-TPA-DBPzCN	H → L (68%) H-1 → L (20%)	6.18	25.88	H-6 → L (93%)	0.48	1.60	H-1 → L (43%) H → L (33%)	4.45	12.77	H-6 → L (91%)	0.17	0.57
4-TPA-DBPzCN	H → L (63%) H-1 → L (24%)	5.54	25.58	H-6 → L (77%)	1.10	3.62	H-6 → L (74%)	0.33	1.05	H-1 → L (49%) H-3 → L (23%)	2.87	7.19

[a] Distance over which charge is transferred between the indicated states upon excitation. [b] Dipole moment change upon excitation.

Table S2. Nature of the various transitions (H = HOMO, L = LUMO), charge-transfer distance (d_{CT}), and change in dipole moment ($\Delta\mu$, excited state dipole – ground state dipole) accompanying the $S_0 \rightarrow T_x$ (x = 3,4,5) transitions in cyclohexane, as determined with TDDFT-TDA and a modified LC-BLYP (ω = 0.17 bohr^{-1}) exchange correlation functional.

Compound	$S_0 \rightarrow T_3$			$S_0 \rightarrow T_4$			$S_0 \rightarrow T_5$		
	Nature	d_{CT} (Å)[a]	Δμ (D)[b]	Nature	d_{CT} (Å)[a]	Δμ (D)[b]	Nature	d_{CT} (Å)[a]	Δμ (D)[b]
1-TPA-DBPzCN	H-6 → L (31%) H-2 → L (29%) H-1 → L (17%)	0.90	1.92	H-3 → L (44%) H-1 → L (20%) H-2 → L (11%)	1.66	4.40	H → L+1 (73%)	3.34	16.24
2-TPA-DBPzCN	H-2 → L (90%)	1.71	4.06	H-5 → L (26%) H → L (23%) H-6 → L (20%)	3.72	9.14	H → L+2 (51%) H → L+6 (14%) H → L+7 (6%)	3.17	8.21
3-TPA-DBPzCN	H-2 → L (60%) H-3 → L (13%)	1.69	3.73	H → L+3 (29%) H-1 → L (17%) H → L+1 (12%) H → L+7 (9%)	4.08	10.77	H-5 → L (19%) H-2 → L (18%) H-9 → L (14%) H-3 → L (14%)	2.23	5.47
4-TPA-DBPzCN	H-2 → L (73%)	2.41	5.96	H → L (36%) H-3 → L (18%) H-2 → L (12%) H-6 → L (6%)	4.89	16.47	H → L+2 (35%) H → L+6 (29%) H → L+3 (5%)	2.92	7.35

[a] Distance over which charge is transferred between the indicated states upon excitation. [b] Dipole moment change upon excitation.

Table S3. TDDFT results for the five vertical singlet excitation energies and the corresponding oscillator strengths (f), and the five vertical triplet excitation energies as determined with TDDFT-TDA and a modified LC-BLYP (ω = 0.17 bohr^{-1}) exchange correlation functional, and the calculated singlet-triplet energy gaps between the first excited singlet state and the specified triplet excited states.

Compound	S_1 (eV) (nm)	f_{S_1}	S_2 (eV) (nm)	f_{S_2}	S_3 (eV) (nm)	f_{S_3}	S_4 (eV) (nm)	f_{S_4}	S_5 (eV) (nm)	f_{S_5}	T_1 (eV)	T_2 (eV)	T_3 (eV)	T_4 (eV)	T_5 (eV)	$\Delta E_{S_1\text{-}T_1}$ (eV)	$\Delta E_{S_1\text{-}T_x}$ (eV)[a]
DBPzCN	3.00 (413)	0.002	3.23 (384)	0.027	/	/	/	/	/	/	2.59	2.64	/	/	/	/	/
1-TPA-DBPzCN	2.23 (556)	0.003	2.93 (423)	0.002	3.05 (407)	0.043	3.27 (379)	0.050	3.29 (377)	0.332	2.09	2.62	2.68	2.81	2.99	0.14	0.14 (x=1)
2-TPA-DBPzCN	2.73 (454)	0.094	3.01 (412)	0.003	3.35 (370)	0.325	3.44 (360)	0.071	3.57 (347)	0.955	2.46	2.59	2.75	2.87	3.03	0.27	0.27 (x=1)
3-TPA-DBPzCN	2.91 (426)	0.779	3.01 (412)	0.009	3.25 (381)	0.170	3.46 (358)	0.148	3.69 (336)	0.985	2.46	2.60	2.69	2.97	3.17	0.45	0.45 (x=1)
4-TPA-DBPzCN	2.91 (426)	0.093	3.01 (412)	0.017	3.28 (378)	0.197	3.39 (366)	0.313	3.68 (337)	0.625	2.59	2.60	2.69	2.91	3.16	0.32	~ 0.00 (x=4)

[a] Smallest positive calculated singlet-triplet energy gap between the first excited singlet state and the lowest excited triplet state of CT nature.

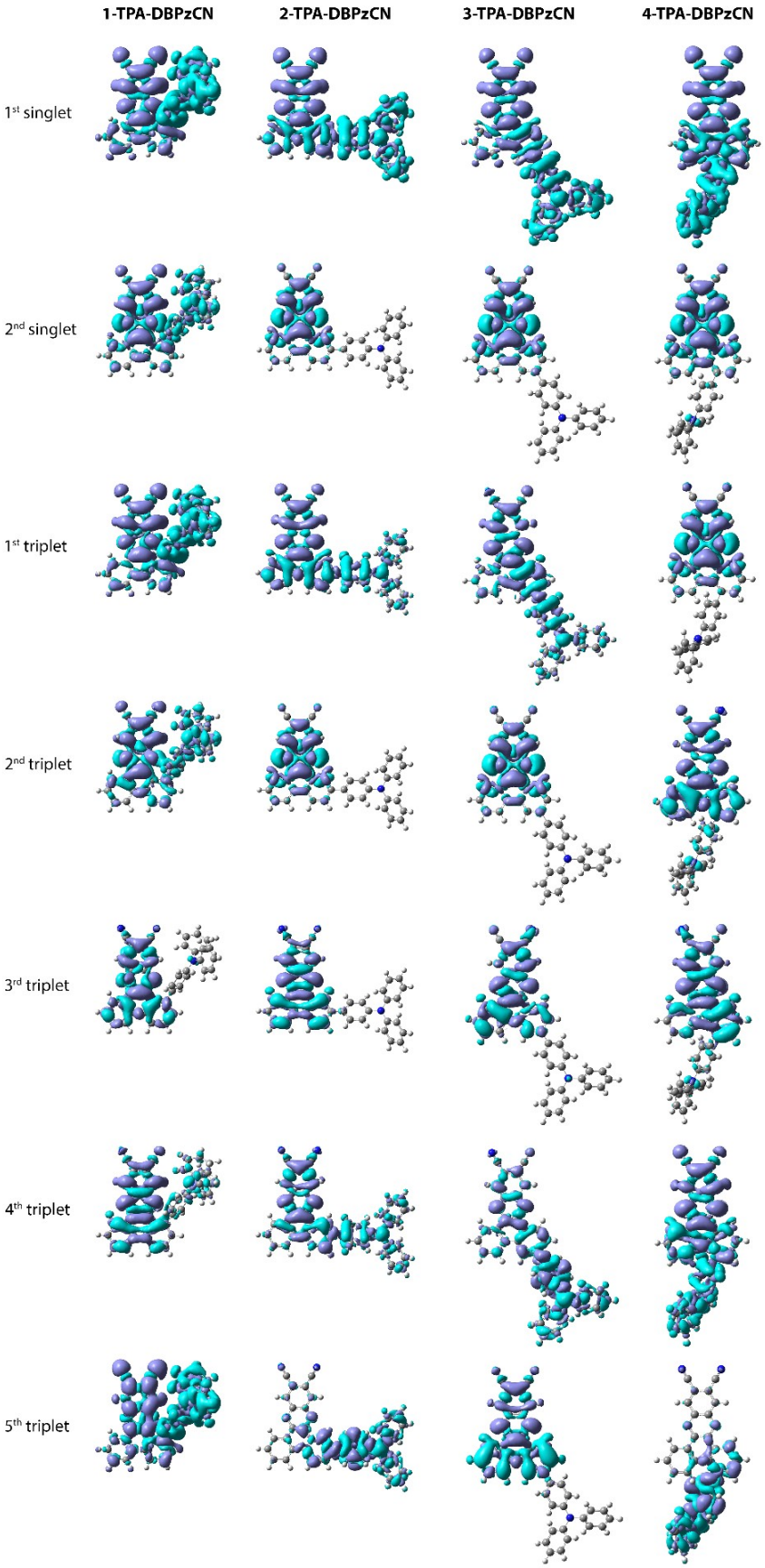

Figure S1: Ground – excited state electron density differences for the singlet and triplet excited states of **DBPzCN**, **1-TPA-DBPzCN**, **2-TPA-DBPzCN**, **3-TPA-DBPzCN**, and **4-TPA-DBPzCN**. Purple areas indicate increased electron density, while cyan areas point to decreased electron density (isosurface value = 0.0004 a.u. for all densities).

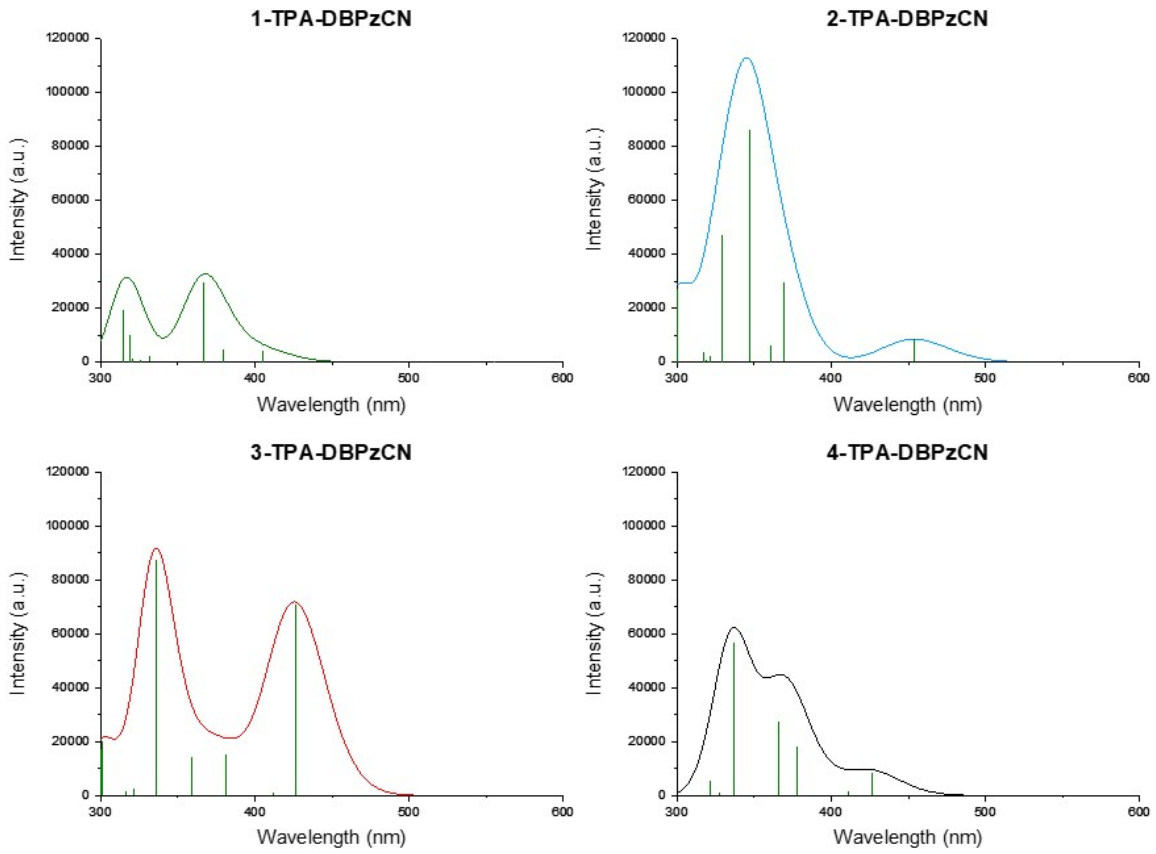

Figure S2: Simulated UV-Vis absorption spectra derived from the TDDFT results for the optimized geometries by fitting the vertical excitation energies with a Gaussian and employing a full-width-at-half-maximum of 0.3 eV for each excitation. The vertical lines indicate the specific excitation energies and their relative size is indicative of the oscillator strength accompanying the transition.

4. Conformation comparison based on TDDFT-optimized molecular geometries

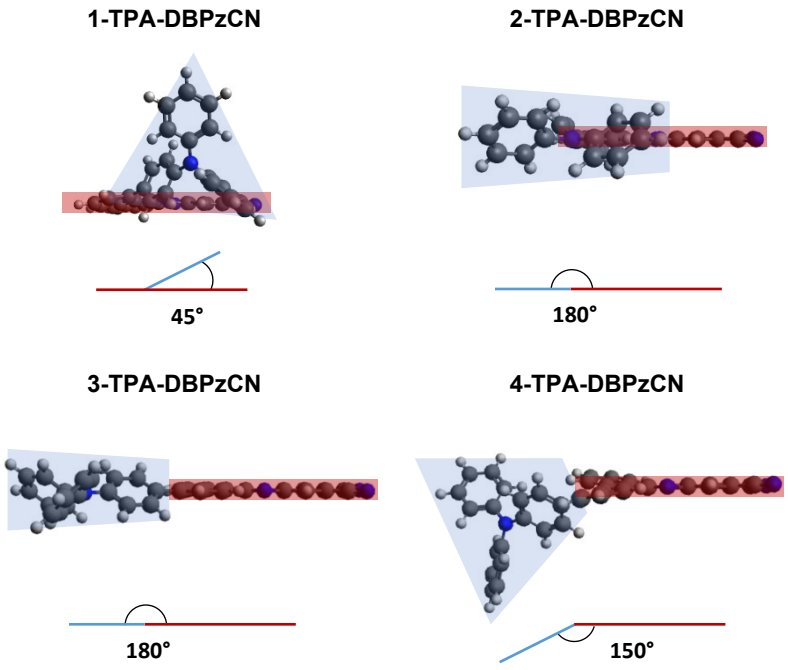

Figure S3: Conformations of the four isomers based on their optimized TDDFT-derived molecular geometry. Structures are coloured in terms of their donor (blue) and acceptor (red) unit and are schematically visualized to indicate the relative orientation and angle between the approximate planes of both units.

5. Photoluminescence and singlet oxygen quantum yields in toluene

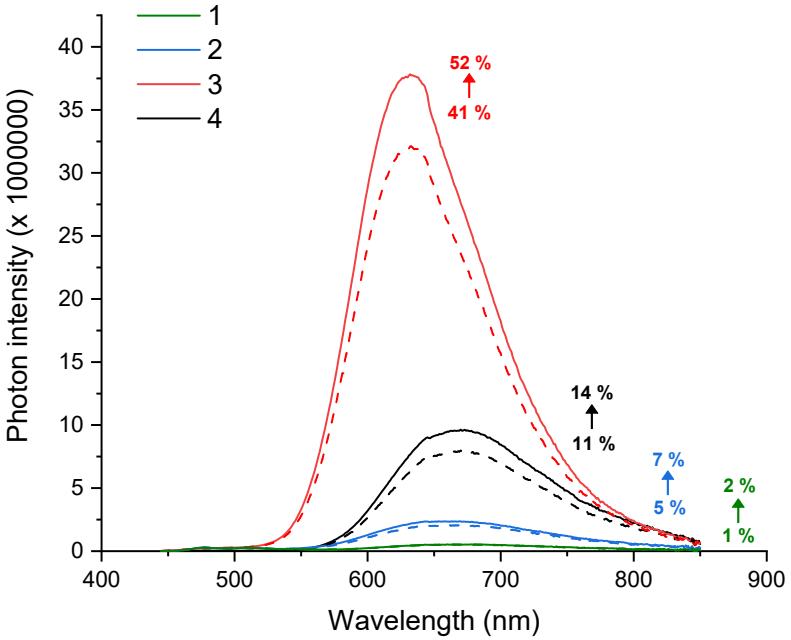

Figure S4: Emission spectra and related photoluminescence quantum yields in toluene obtained for the four emitters in air (dashed lines) and in inert atmosphere (solid lines).

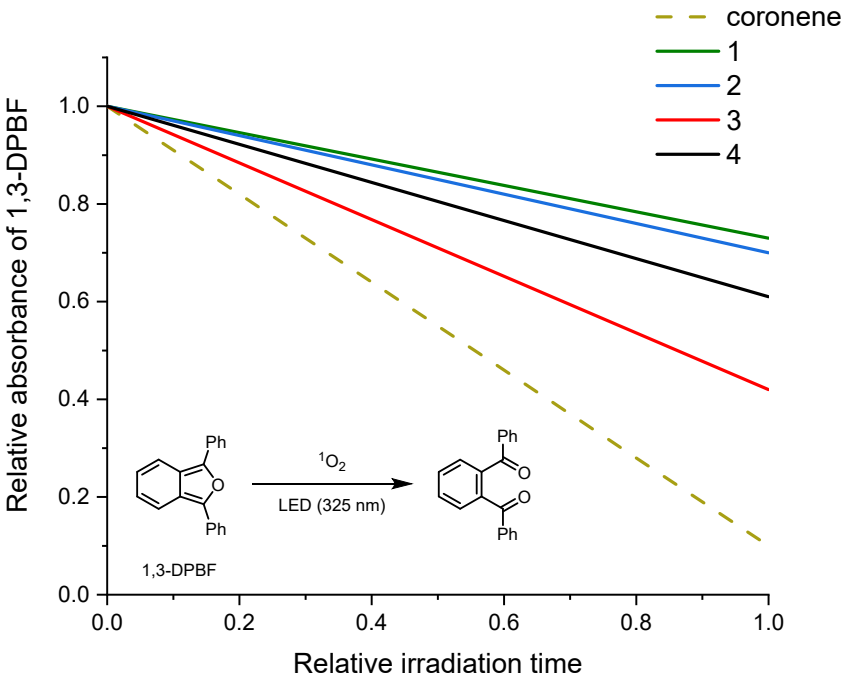

Figure S5: Relative decrease in absorbance of 1,3-diphenylisobenzofuran at 414 nm under continuous irradiation using a single 325 nm LED in the presence of the respective emitter in toluene. Coronene was used as a standard (Φ_Δ = 0.90 in toluene).

6. Solution state absorption and emission spectra for solvatochromism determination

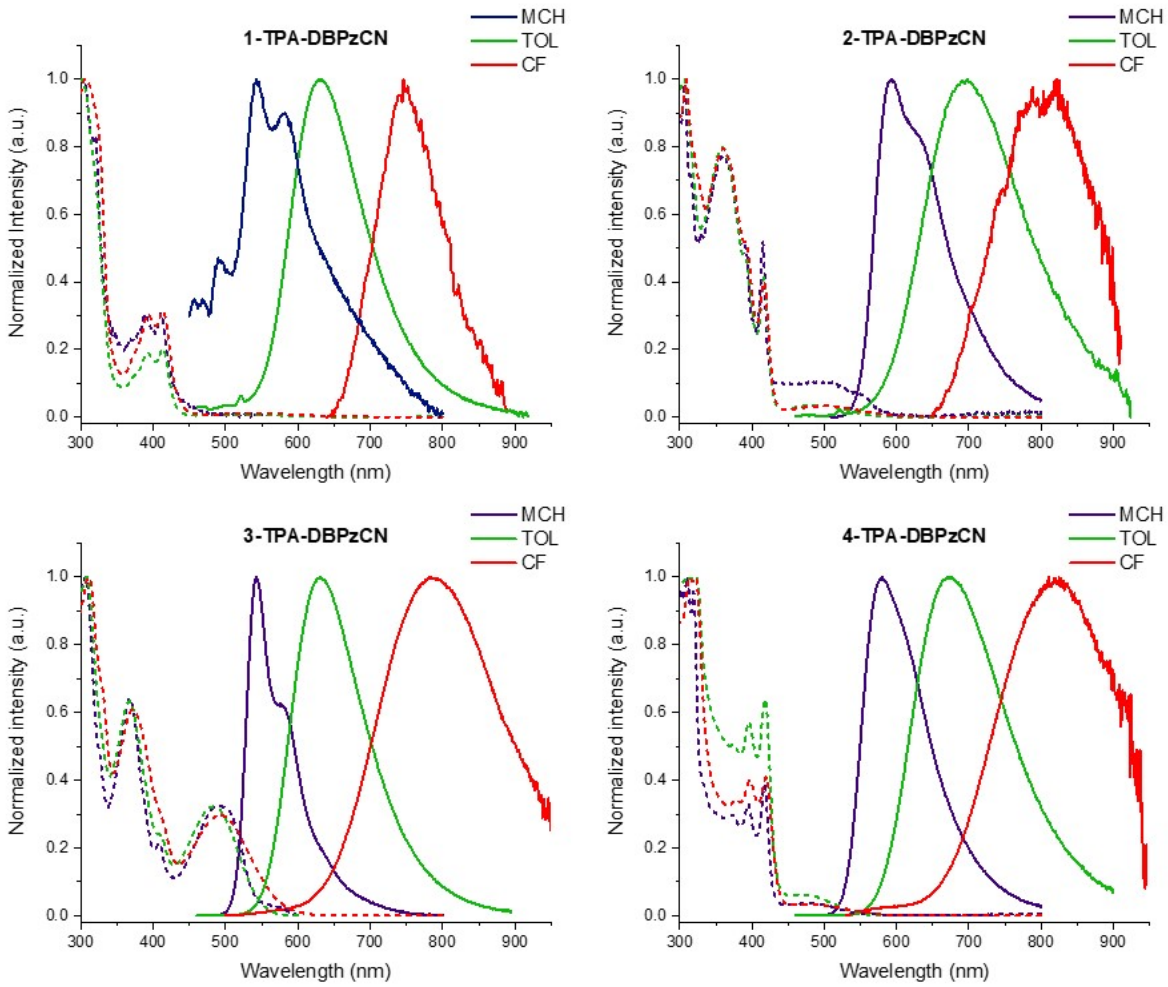

Figure S6: Normalized steady-state absorption spectra (dashed lines) and emission spectra (solid lines) for the four emitters in methylcyclohexane (MCH, blue), toluene (TOL, green) and, chloroform (CF, red). The fine-structure below 530 nm in the emission spectrum of **1-TPA-DBPzCN** in MCH can be attributed to the presence of a residual Raman peak.

Table S4. Absorption and emission peak maxima for the four emitters in solution.

Compound	$\lambda_{CT\ abs}$ (nm)[a]			λ_{em} (nm)[b]		
	MCH	TOL	CF	MCH	TOL	CF
1-TPA-DBPzCN	531	536	550	535,592	632	745
2-TPA-DBPzCN	494	495	504	593,632	694	805
3-TPA-DBPzCN	491	484	493	542,578	630	786
4-TPA-DBPzCN	486	480	490	579	672	819

[a] Absorption maxima for the CT band in methylcyclohexane (MCH), toluene (TOL), and chloroform (CF) solution. [b] Fluorescence emission maxima in MCH, TOL, and CF solution (10^{-5} M).

7. Cyclic voltammetry and HOMO/LUMO determination

Cyclic voltammetry experiments were performed to determine the HOMO and LUMO energies of the isomer materials. Since each structure shares the same donor and acceptor unit, these values are expected to be relatively similar. Both **1-** and **4-TPA-DBPzCN** show slightly shifted values (HOMO/LUMO for **1** and LUMO for **4**) when compared to **2-** and **3-TPA-DBPzCN**, which is likely related to the twisted conformation of their TPA unit. Interestingly, a significant change in the shape of the cyclic voltammogram can be observed between the initial (1st) and the later (e.g. 5th) oxidation scans (**Figure S7**). This is a result of dimerization (and possible further electropolymerization) following oxidation, which is sometimes observed for TPA derivatives.[9] This oxidative coupling occurs due to the rotational freedom of the TPA unit**,** which can prevent stabilization through electron delocalization to the acceptor unit (**Figure S8**).[10] For this reason, the onset potential of the first oxidation scan was used to determine the HOMO and LUMO values in **Table 1**. Values based on later scans can be found in **Table S5**.

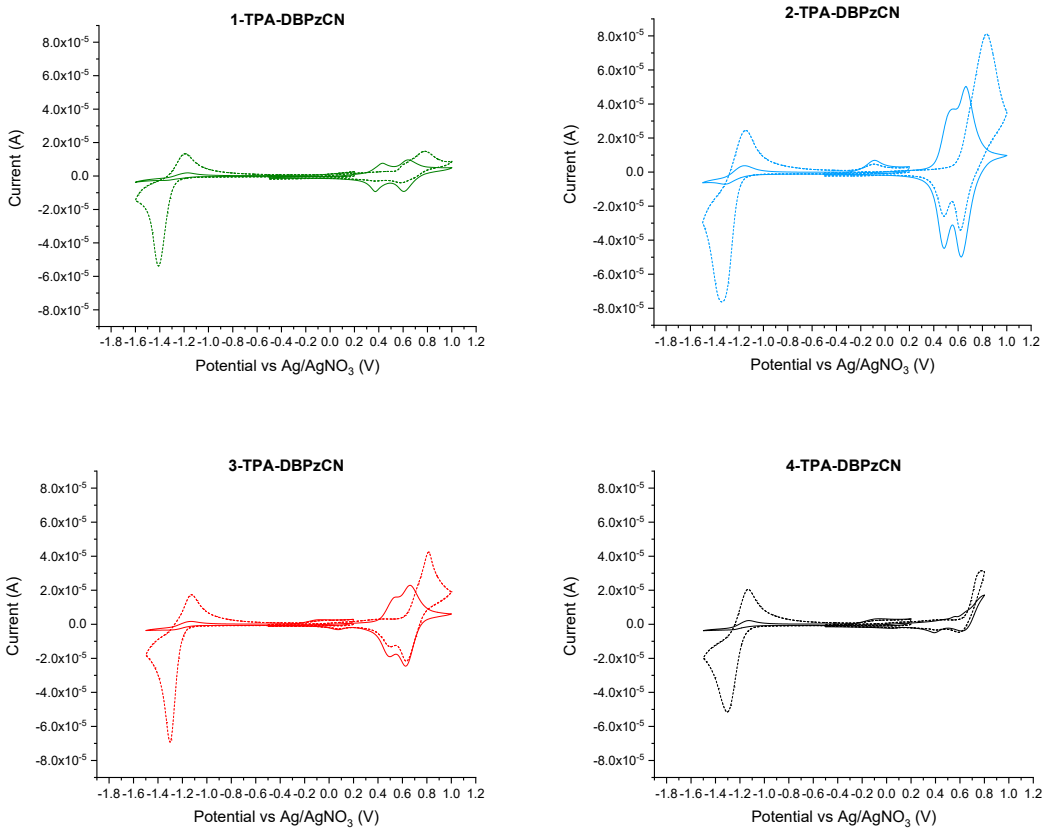

Figure S7: Cyclic voltammograms for the four isomers determined in acetonitrile at room temperature with $TBAPF_6$ as supporting electrolyte. Combined oxidation and reduction voltammograms of the 1st scan (dotted line) and 5th scan (solid line) are shown.

Table S5. Experimental HOMO/LUMO values derived from cyclic voltammetry.

Compound	HOMO/LUMO (eV)[a] 1st ox/red scan	HOMO/LUMO (eV)[b] 5th ox/red scan
1-TPA-DBPzCN	-5.45/-3.61	-5.17/-3.61
2-TPA-DBPzCN	-5.51/-3.71	-5.31/-3.71
3-TPA-DBPzCN	-5.54/-3.69	-5.32/-3.69
4-TPA-DBPzCN	-5.57/-3.75	/[c]

[a] Values estimated from the oxidation and reduction onset potentials of the 1st scan. [b] Values estimated from the average oxidation and reduction onset potentials of the 3rd, 4th, and 5th scan. [c] No accurate values could be determined due to the poor signal and large discrepancies between scans.

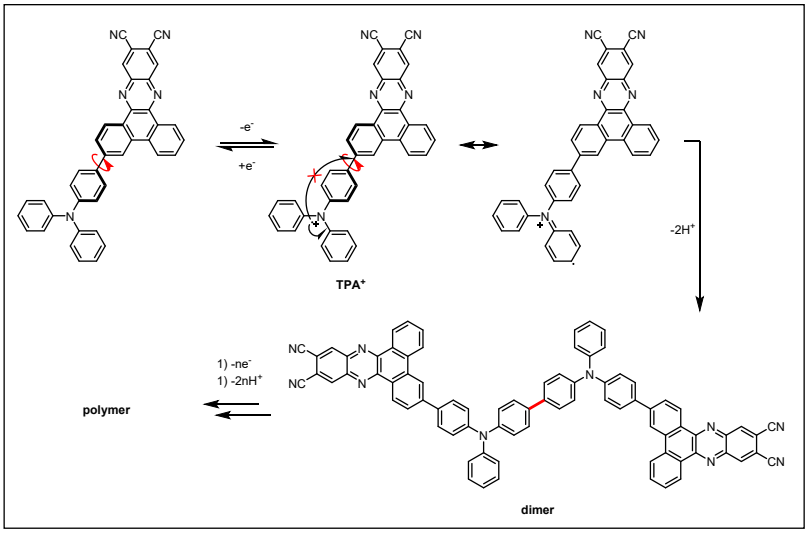

Figure S8: Proposed oxidation and electrochemical oxidative coupling reaction of the TPA-containing isomers, illustrated for **3-TPA-DBPzCN**.[10]

8. Single-crystal X-ray crystallography

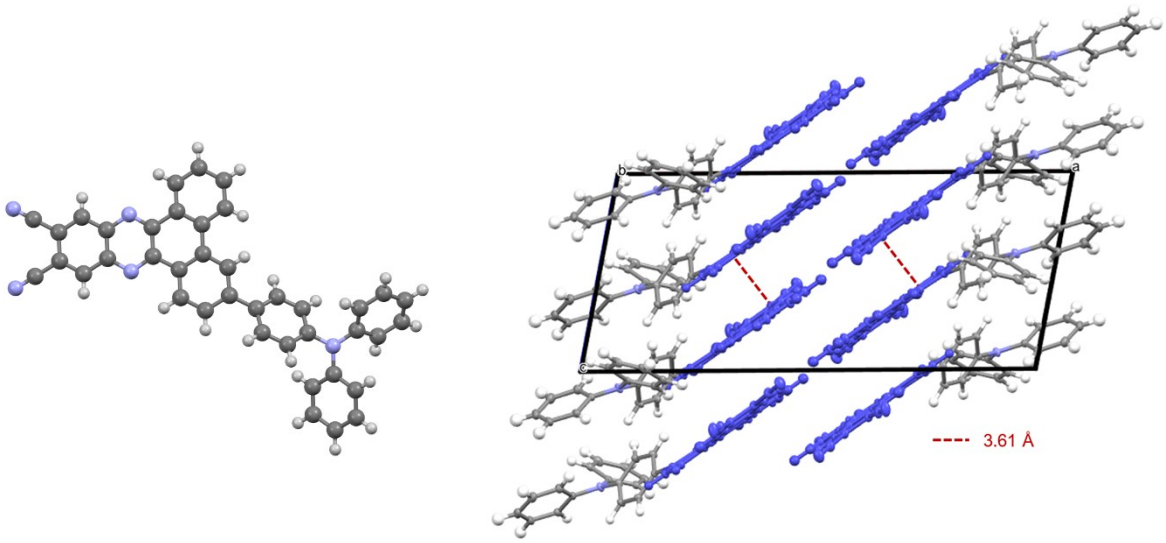

Figure S9: Single crystal configuration (left) and single crystal packing mode (right) of **3-TPA-DBPzCN**. For the single crystal packing mode, the **DBPzCN** acceptor unit is pictured in blue.

Table S6. Crystallographic data of **3-TPA-DBPzCN**.

Compound	3-TPA-DBPzCN
CCDC number	2354499
Identification code	22srv363
Empirical formula	$C_{40}H_{23}N_5$
Formula weight	573.63
Temperature/K	120.00
Crystal system	monoclinic
Space group	$P2_1/c$
a/Å	21.6902(8)
b/Å	13.9625(5)
c/Å	9.5810(4)
α/°	90
β/°	101.1281(15)
γ/°	90
Volume/Å^3	2847.04(19)
Z	4
ρ_{calc}g/cm^3	1.338
μ/mm^{-1}	0.080
F(000)	1192.0
Crystal size/mm^3	0.27 × 0.19 × 0.06
Radiation	Mo Kα (λ = 0.71073)
2Θ range for data collection/°	3.828 to 60
Index ranges	-30 ≤ h ≤ 30, -19 ≤ k ≤ 19, -13 ≤ l ≤ 13
Reflections collected	102101
Independent reflections	8296 [R_{int} = 0.0581, R_{sigma} = 0.0265]
Data/restraints/parameters	8296/0/498
Goodness-of-fit on F^2	1.091
Final R indexes [I>=2σ (I)]	R_1 = 0.0537, wR_2 = 0.1250

9. Solid state emission spectra in CBP and DPEPO hosts

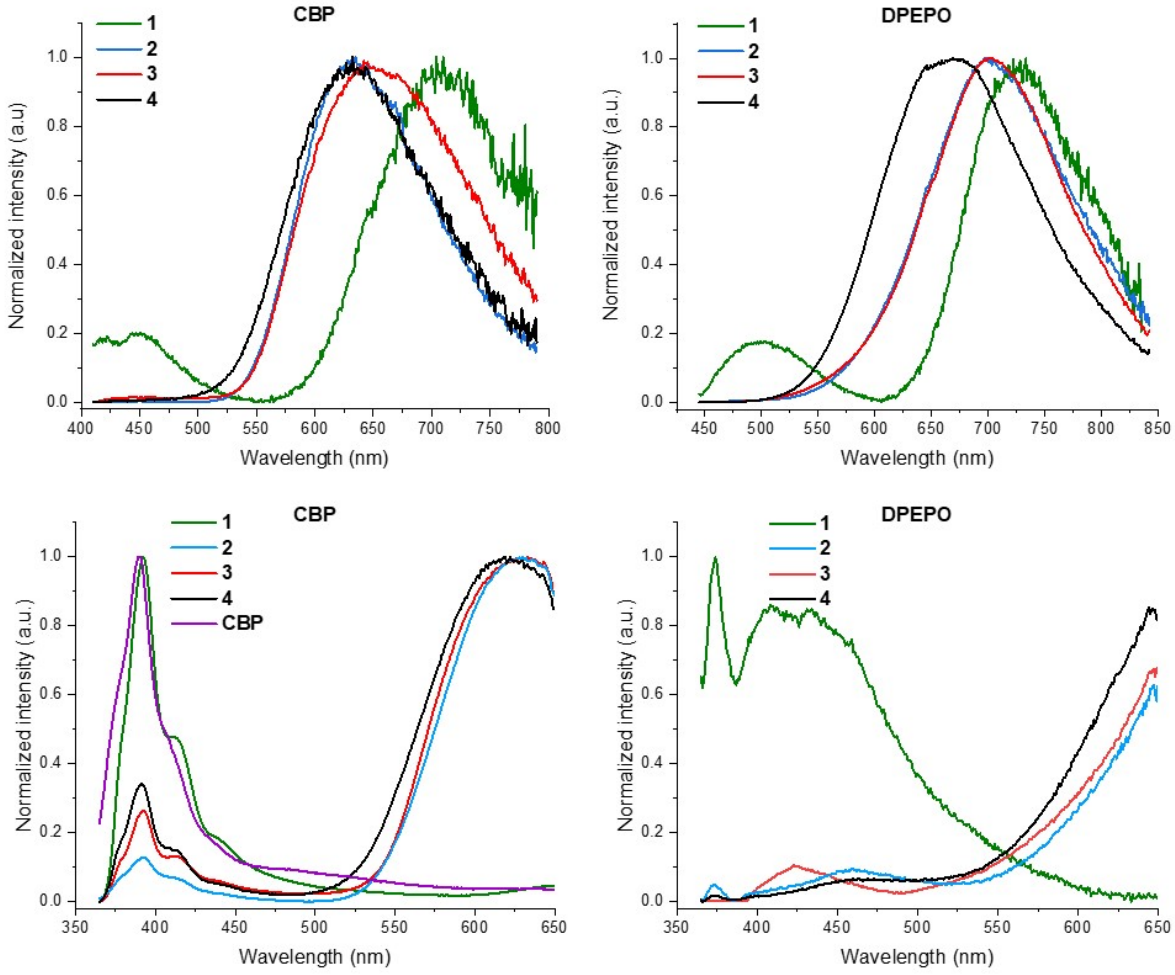

Figure S10: Normalized steady-state emission spectra for all isomers in 1 w/w% CBP (left) and 1 w/w% DPEPO (right) solid films at an excitation wavelength of 400 (top left), 450 (top right) and, 350 nm (bottom).

10. Normalized time-resolved emission spectra (contour plots)

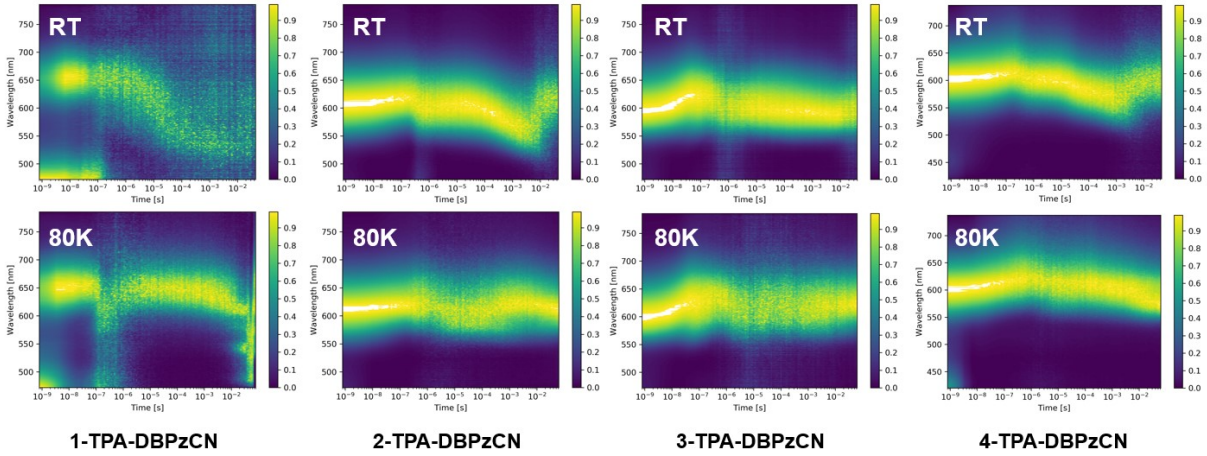

Figure S11: Normalized time-resolved emission spectra (contour plots) for all isomers in 1 w/w% CBP films at room temperature (top row) and at 80 K (bottom row).

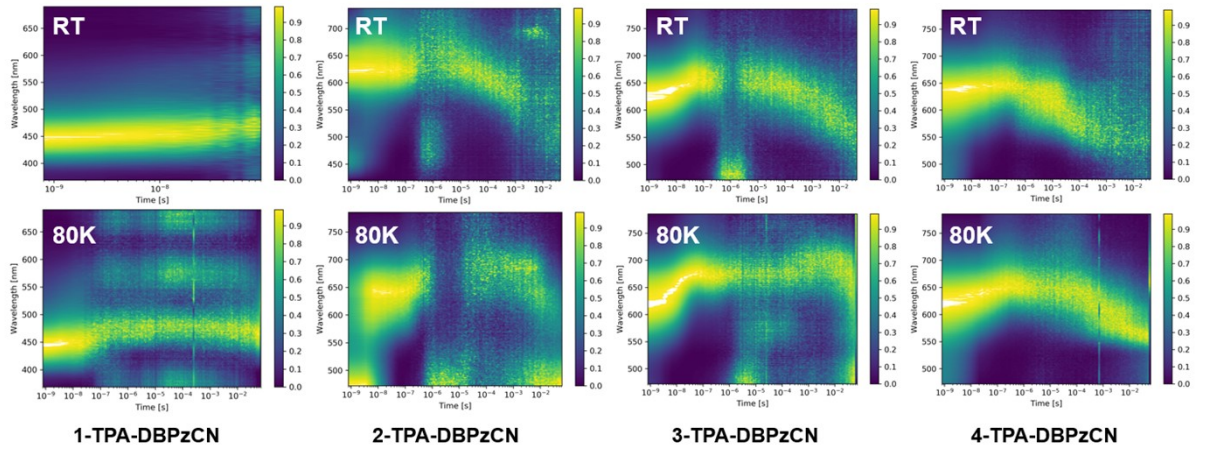

Figure S12: Normalized time-resolved emission spectra (contour plots) for all isomers in 1 w/w% DPEPO films at room temperature (top row) and at 80 K (bottom row).

11. Energy gap determination from steady-state fluorescence and phosphorescence spectra

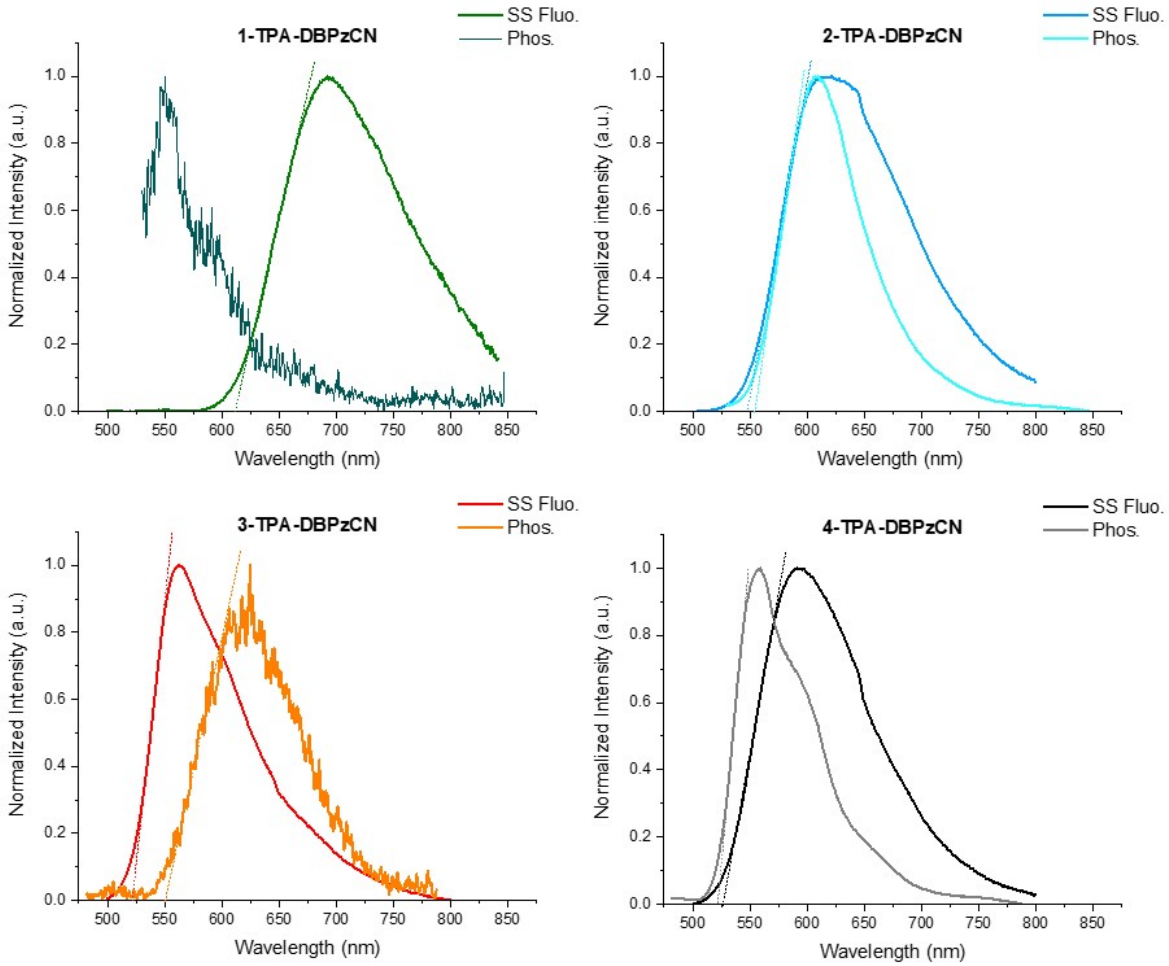

Figure S13: Experimental singlet-triplet energy gap determination via the comparison of steady-state fluorescence spectra at room temperature and 80-milliseconds delay-time phosphorescence spectra at 80 K for the four emitters in 0.1% zeonex films. The irregular spectral shape around 650 nm in the fluorescence spectra of all four isomers can be attributed to the correction file of the spectrofluorometer setup at this wavelength.

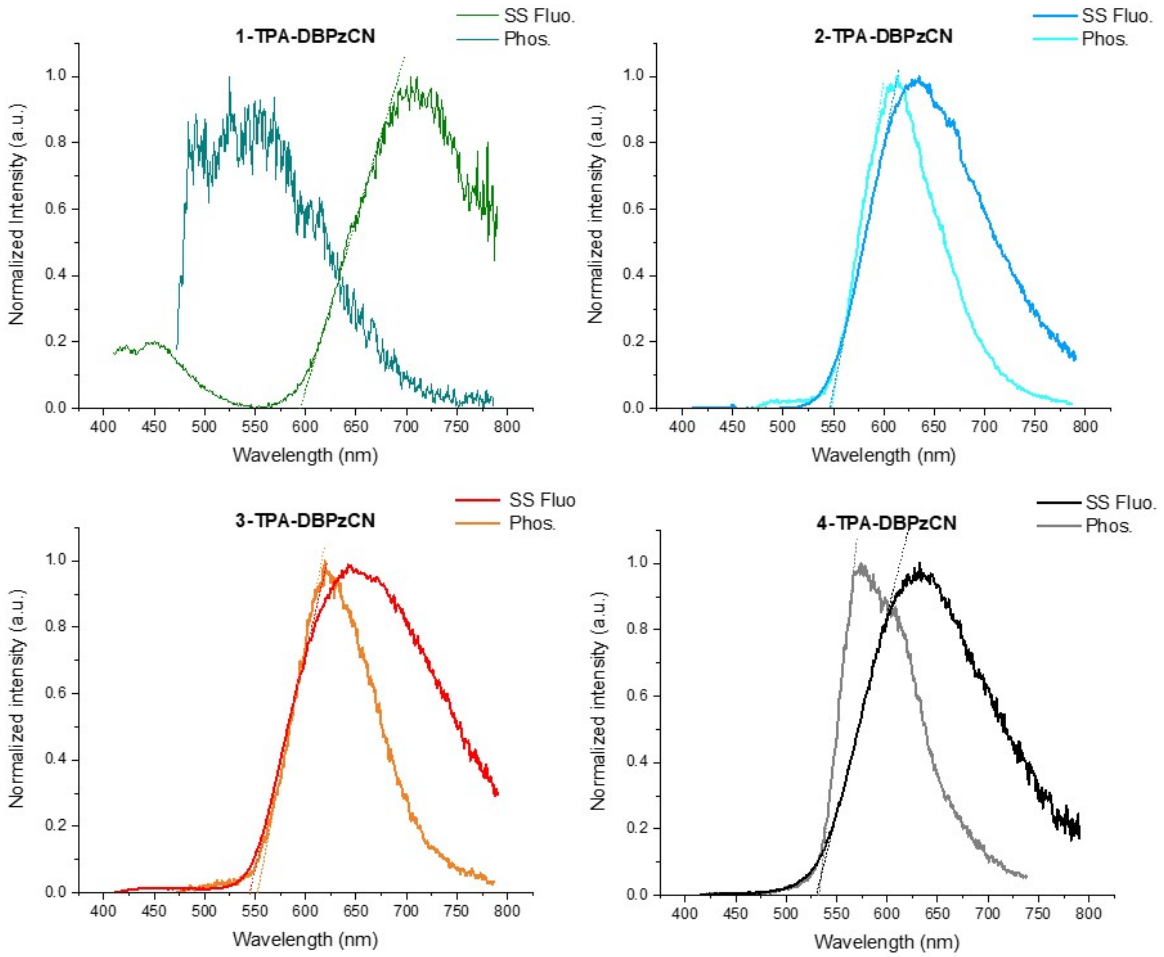

Figure S14: Experimental singlet-triplet energy gap determination via the comparison of steady-state fluorescence spectra at room temperature and 80-milliseconds delay-time phosphorescence at 80 K for the four emitters in 1% CBP films. The irregular spectral shape around 650 nm in the fluorescence spectra of all four isomers can be attributed to the correction file of the spectrofluorometer setup at this wavelength.

12. Total emission decay curves of the four isomers in CBP and DPEPO hosts

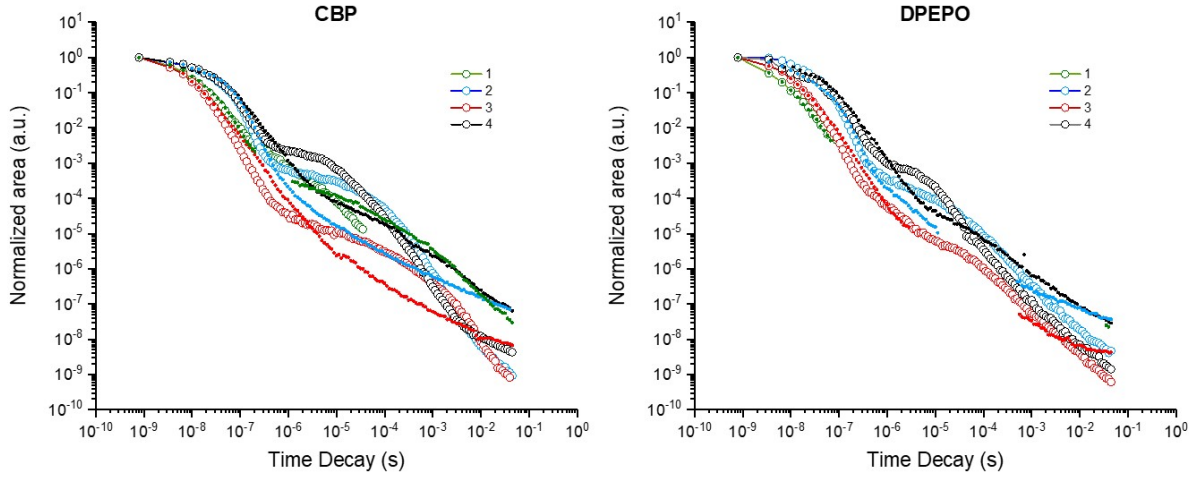

Figure S15: Total emission decay (calculated via the integrated area under the emission curve) for **1-TPA-DBPzCN** (green), **2-TPA-DBPzCN** (blue), **3-TPA-DBPzCN** (red), and **4-TPA-DBPzCN** (black) at room temperature (open circles) and 80 K (closed circles) in CBP (left) and DPEPO (right). Data points with signal below the noise baseline have been omitted from the figure.

Table S7. Experimental singlet-triplet gap and derived kinetic properties of the four emitters in CBP and DPEPO hosts.

Compound	ΔE_{ST} (eV)[a]	k_F (10^7 s^{-1})[b]		k_{ISC} (10^6 s^{-1})[b]		k_{rISC} (10^5 s^{-1})[b]	
	CBP	CBP	DPEPO	CBP	DPEPO	CBP	DPEPO
1-TPA-DBPzCN	/[c]	1.96	/[d]	/[e]		/[e]	
2-TPA-DBPzCN	0.007	1.31	1.74	9.02	3.36	0.60	0.64
3-TPA-DBPzCN	0.031	1.87	2.64	8.36	3.48	0.14	0.17
4-TPA-DBPzCN	0.011	0.85	1.28	10.7	4.35	1.28	1.26

[a] Determined by taking the difference of the onset of the steady-state fluorescence band at room temperature and the 80-milliseconds delay-time phosphorescence band at 80 K. [b] Derived by applying a kinetic fitting model to the total emission decay curves. [c] Could not be determined due to absence of measurable phosphorescence. [d] Could not be accurately determined due to weak prompt fluorescence intensity. [e] Could not be determined due to the absence of measurable delayed fluorescence.

13. Photographs of the emitters in toluene, zeonex, and DPEPO

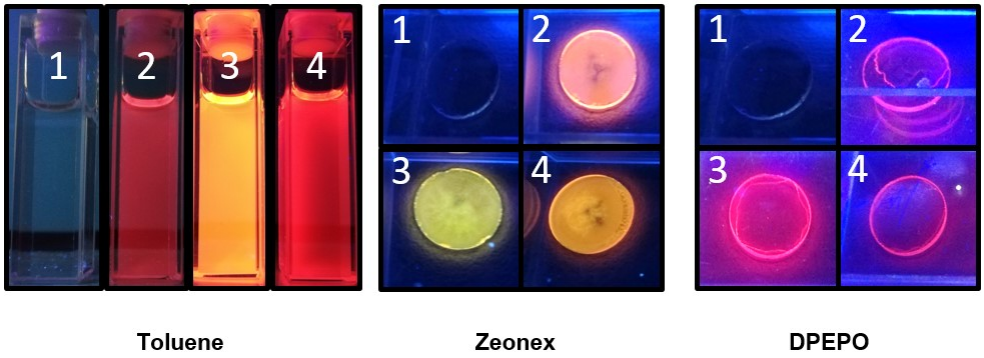

Figure S16: Photographs of the emitters in toluene solution (left), 0.1 w/w% zeonex film (middle), and 1 w/w% DPEPO film (right) upon UV excitation (λ_{exc} = 365 nm).

14. NMR & MALDI-ToF mass spectra

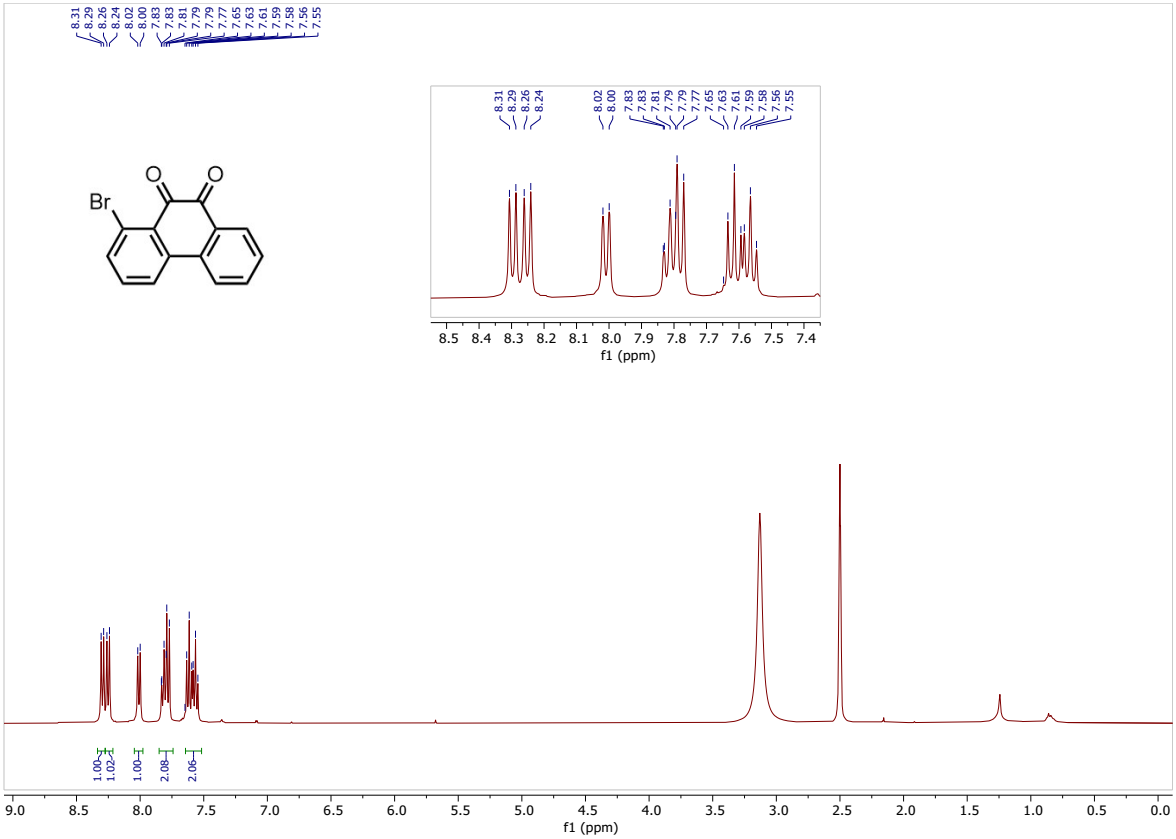

Figure S17: ^{1}H NMR spectrum of 1-bromophenanthrene-9,10-dione (**2-1**) in DMSO-d_6.

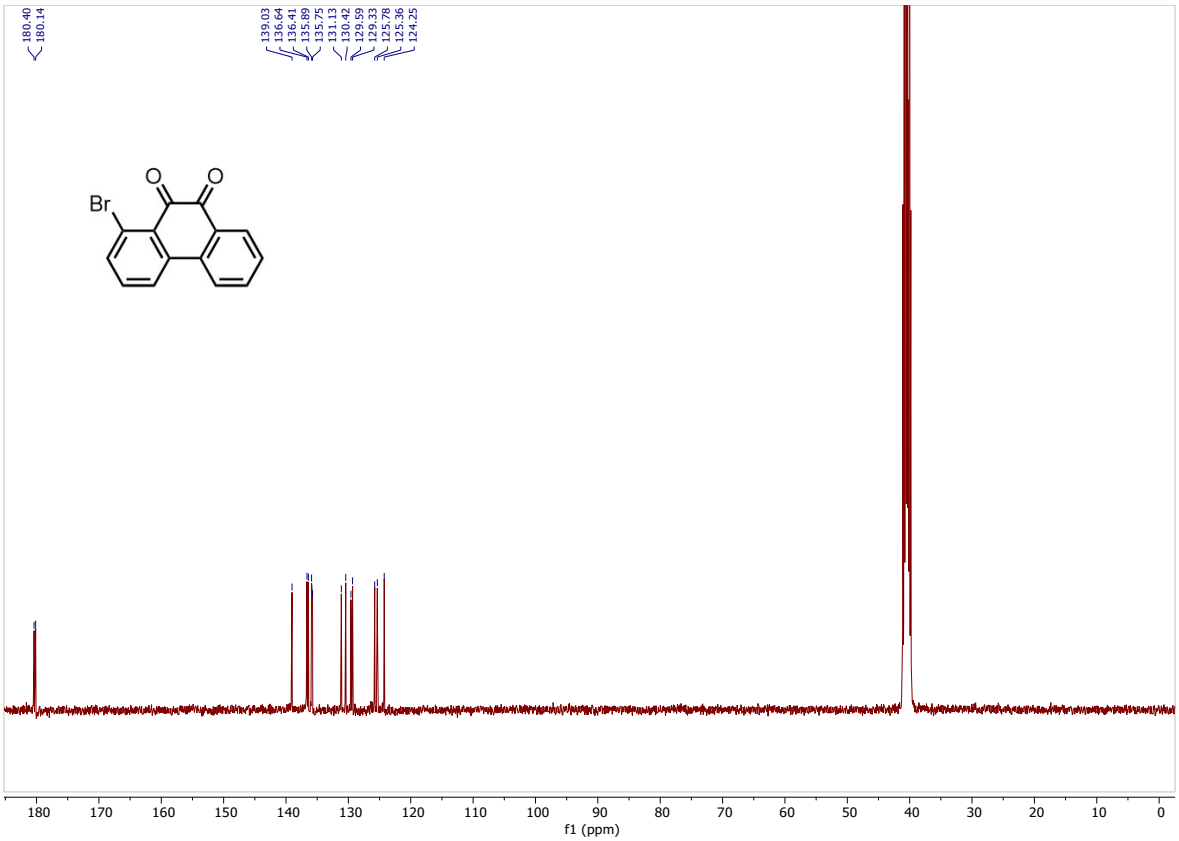

Figure S18: ^{13}C NMR spectrum of 1-bromophenanthrene-9,10-dione (**2-1**) in DMSO-d_6.

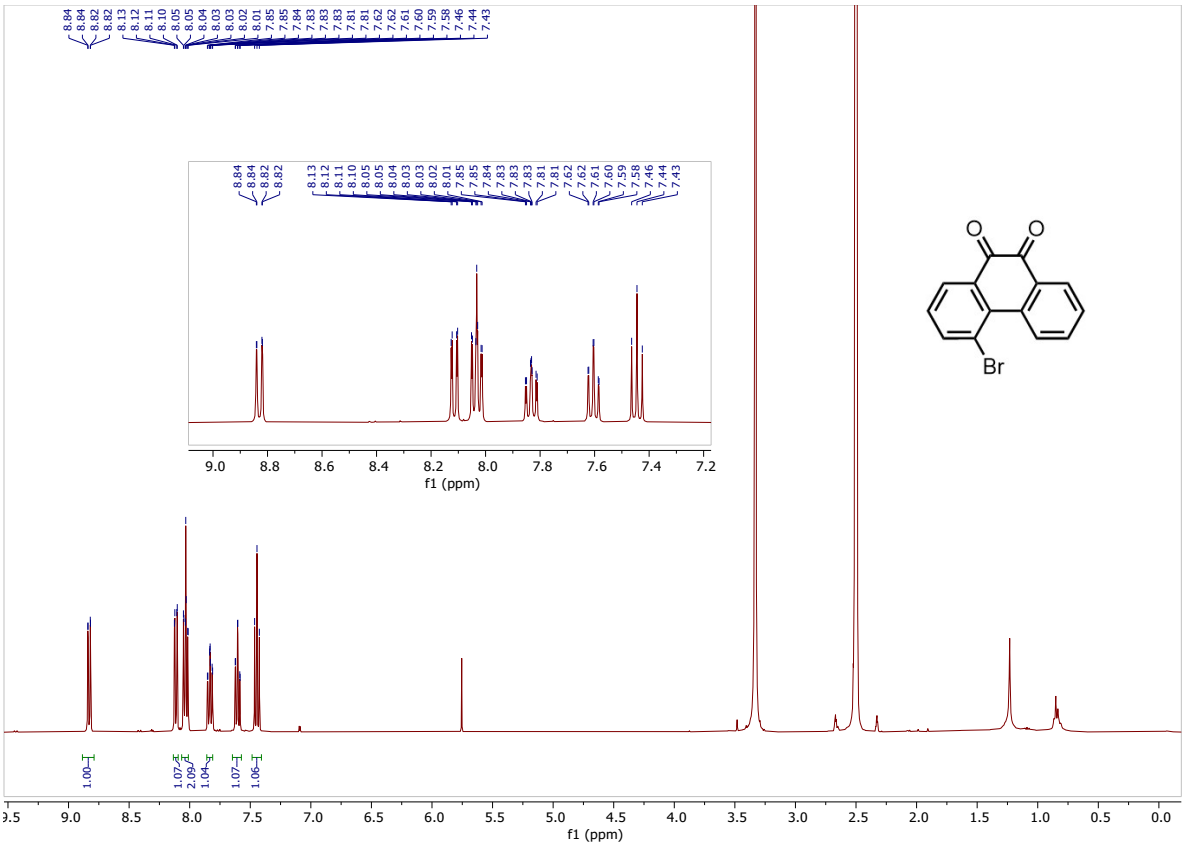

Figure S19: ^{1}H NMR spectrum of 4-bromophenanthrene-9,10-dione (**2-4**) in DMSO-d_6.

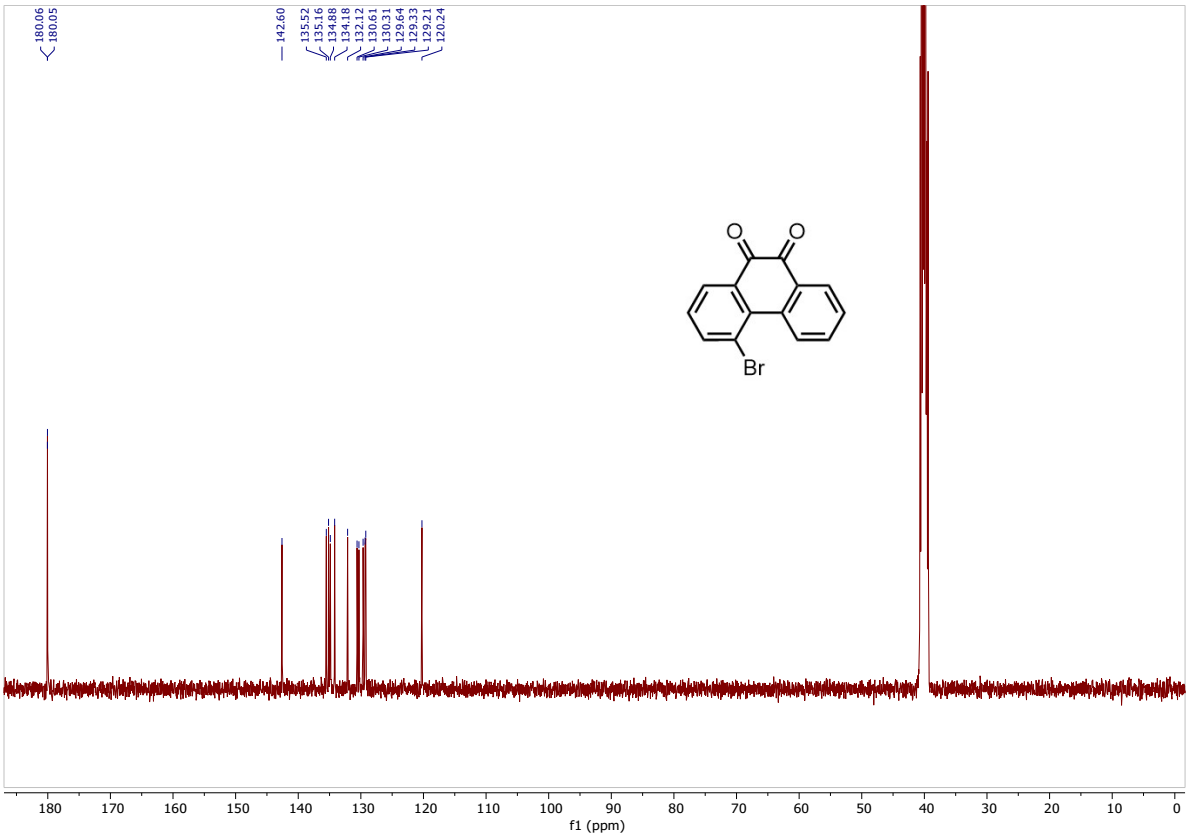

Figure S20: ^{13}C NMR spectrum of 4-bromophenanthrene-9,10-dione (**2-4**) in DMSO-d_6.

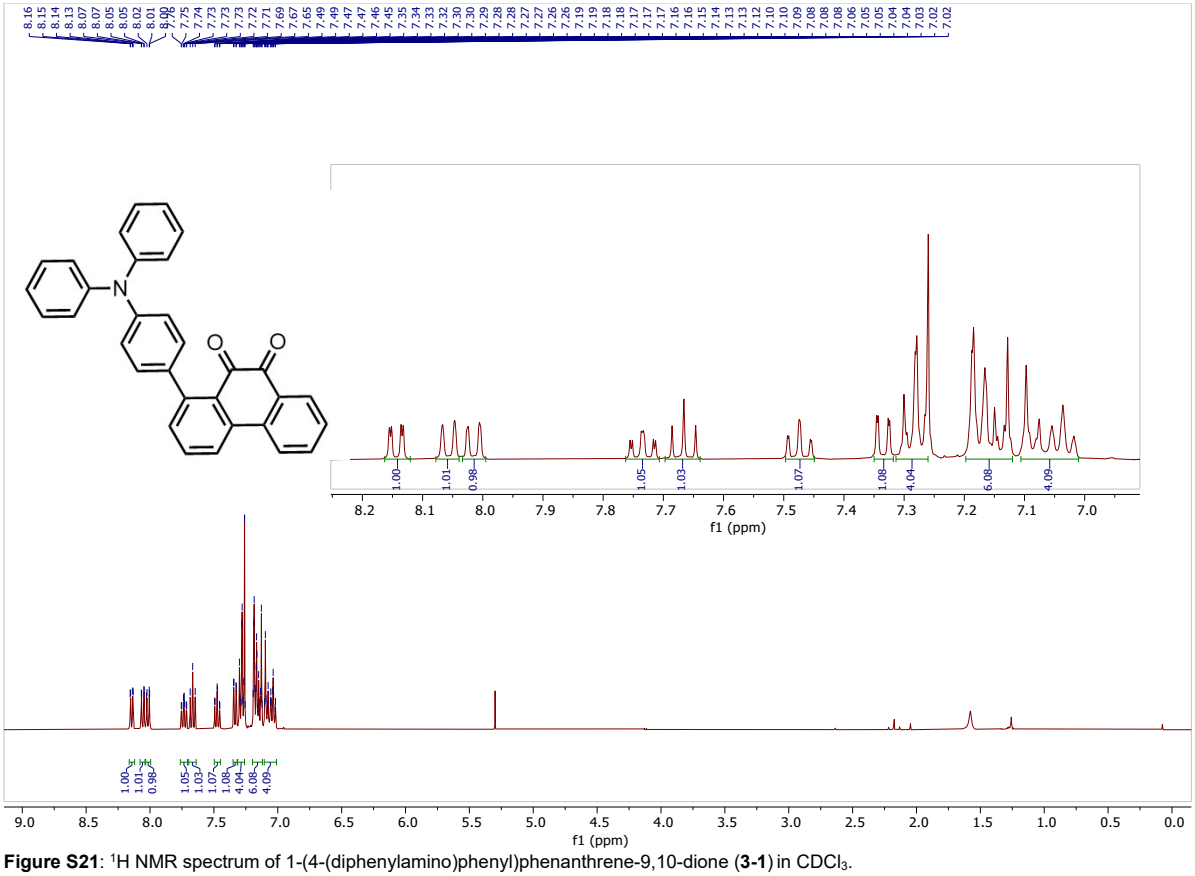

Figure S21: ^{1}H NMR spectrum of 1-(4-(diphenylamino)phenyl)phenanthrene-9,10-dione (**3-1**) in $CDCl_3$.

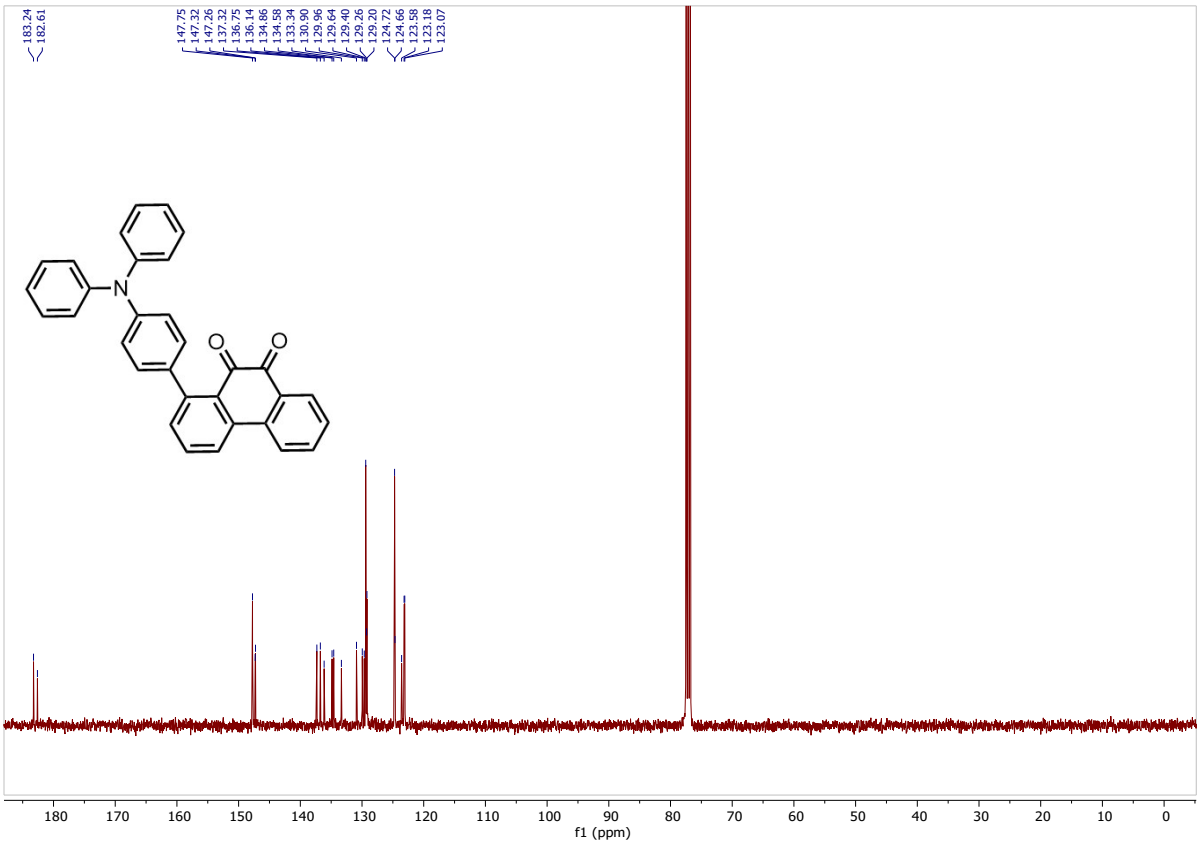

Figure S22: ^{13}C NMR spectrum of 1-(4-(diphenylamino)phenyl)phenanthrene-9,10-dione (**3-1**) in $CDCl_3$.

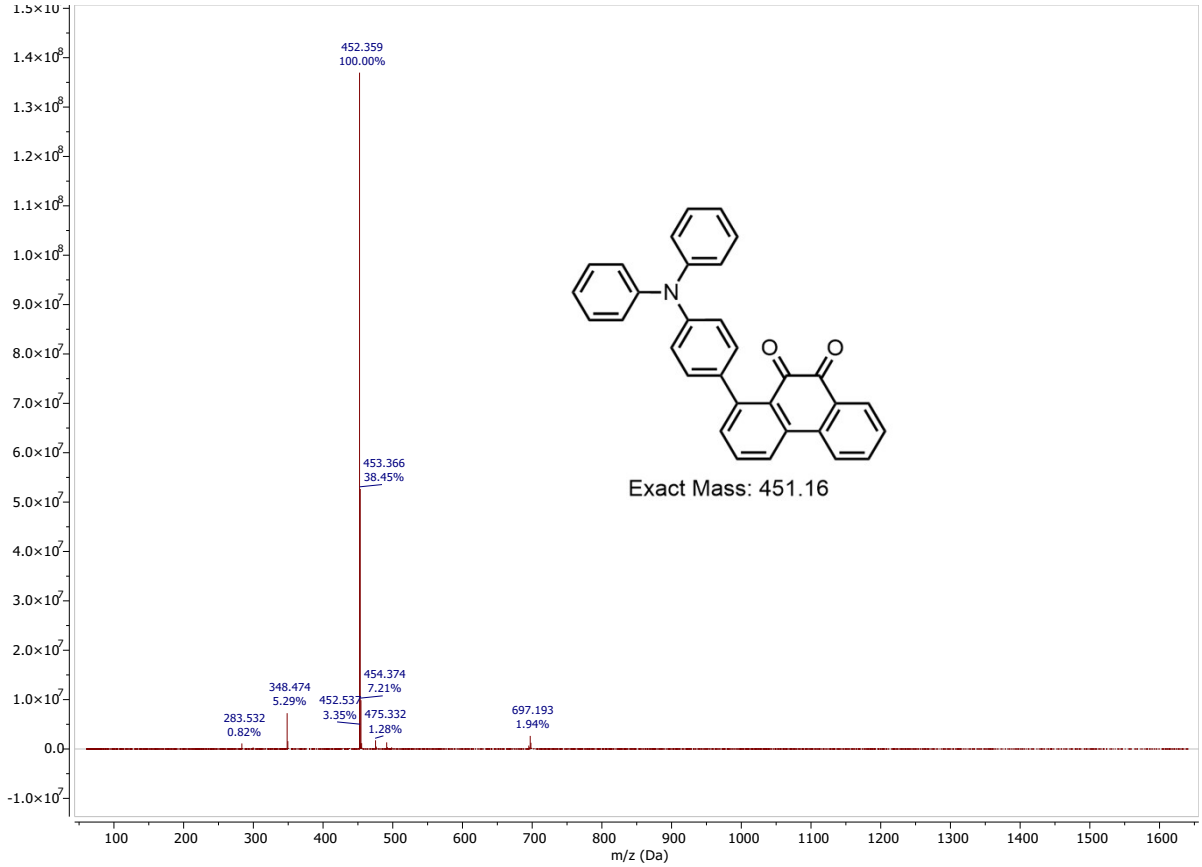

Figure S23: MALDI-ToF mass spectrum of 1-(4-(diphenylamino)phenyl)phenanthrene-9,10-dione (**3-1**).

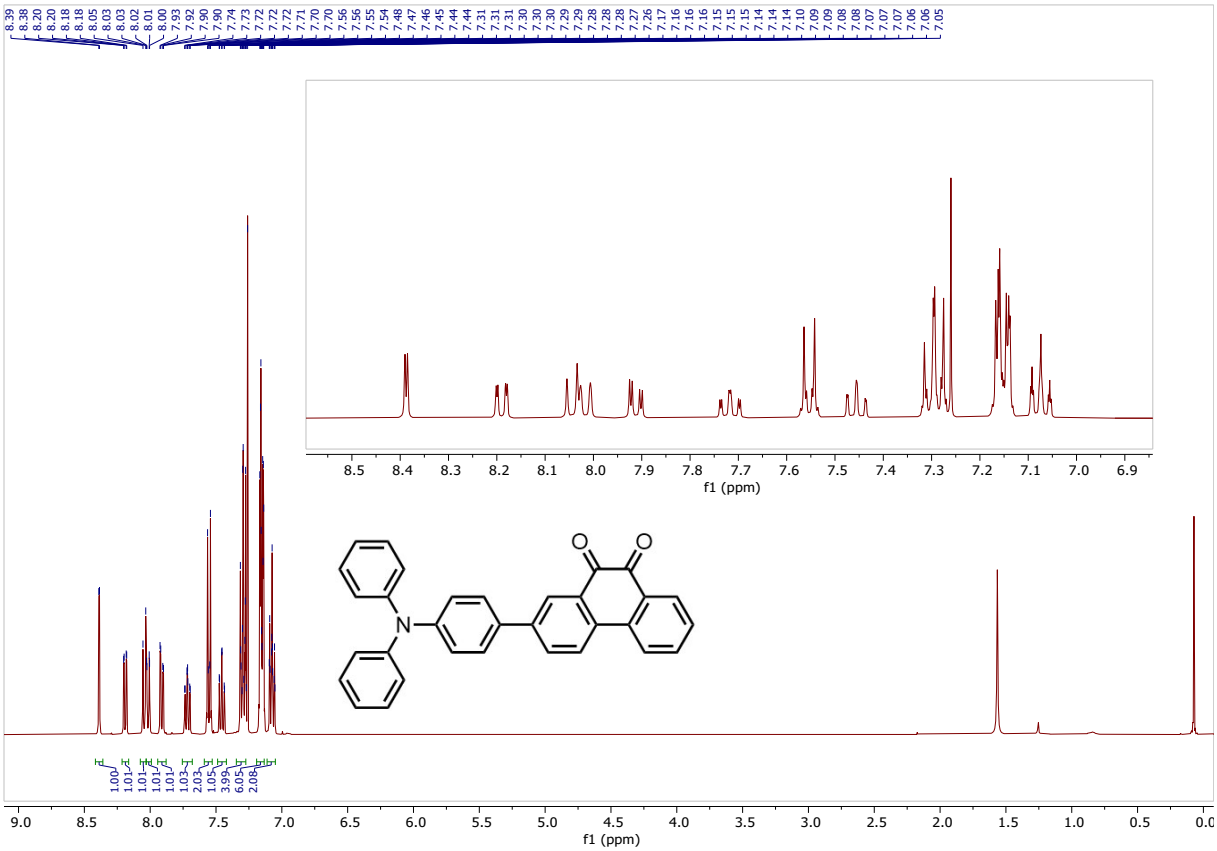

Figure S24: ^{1}H NMR spectrum of 2-(4-(diphenylamino)phenyl)phenanthrene-9,10-dione (**3-2**) in $CDCl_3$.

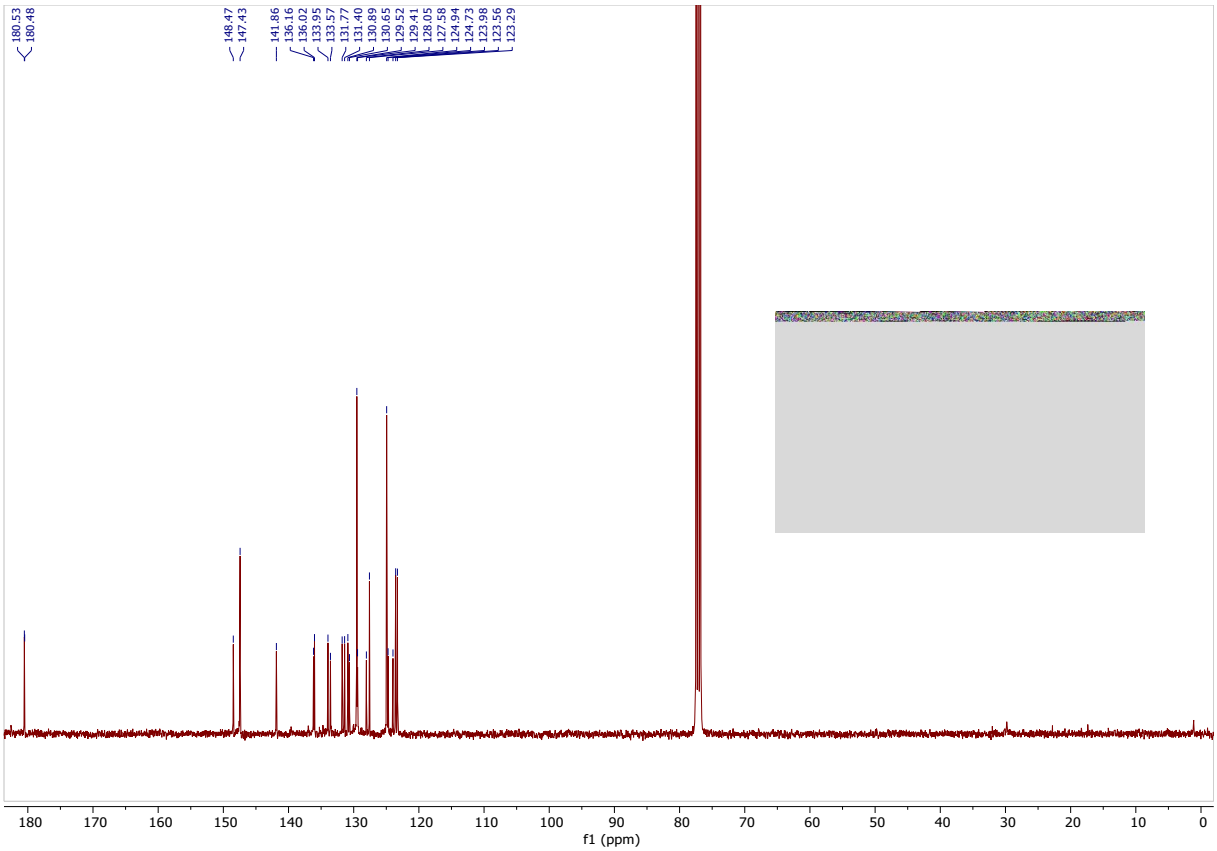

Figure S25: ^{13}C NMR spectrum of 2-(4-(diphenylamino)phenyl)phenanthrene-9,10-dione (**3-2**) in $CDCl_3$.

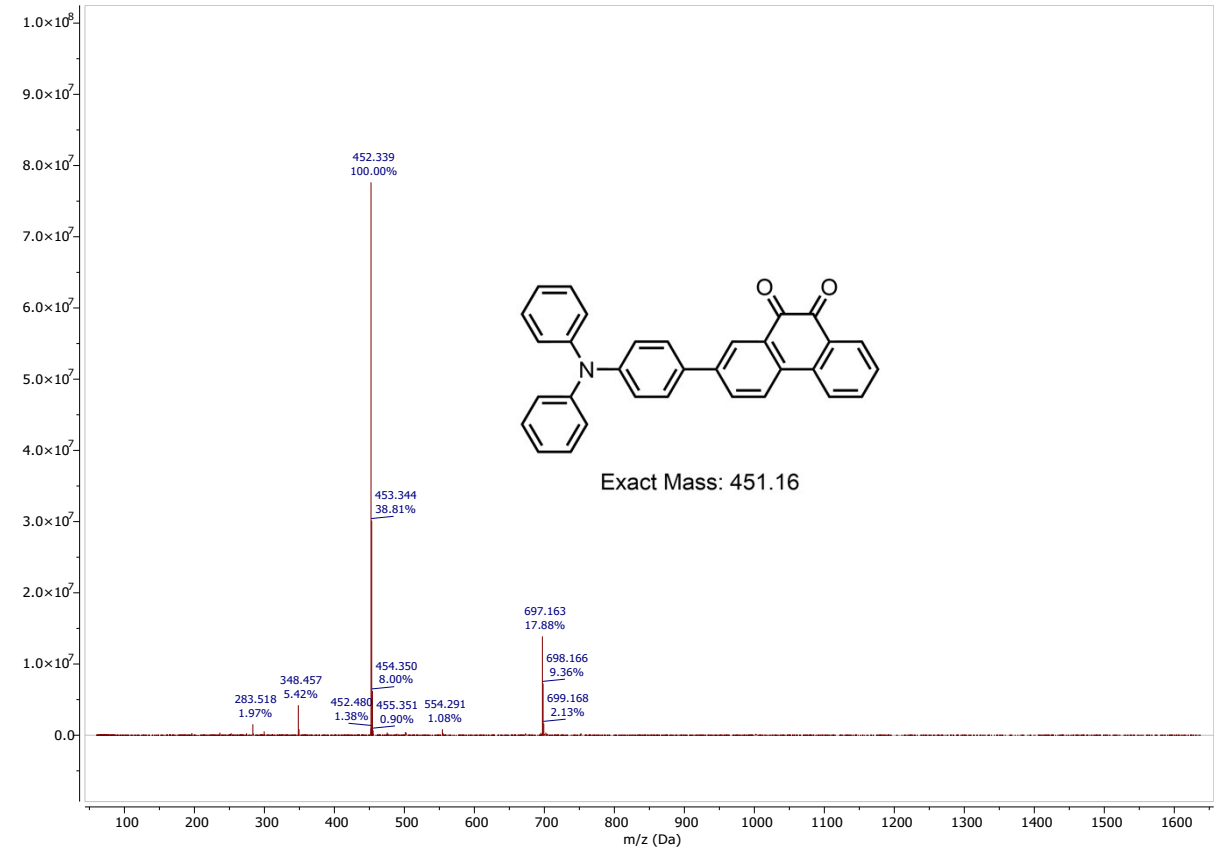

Figure S26: MALDI-ToF mass spectrum of 2-(4-(diphenylamino)phenyl)phenanthrene-9,10-dione (**3-2**).

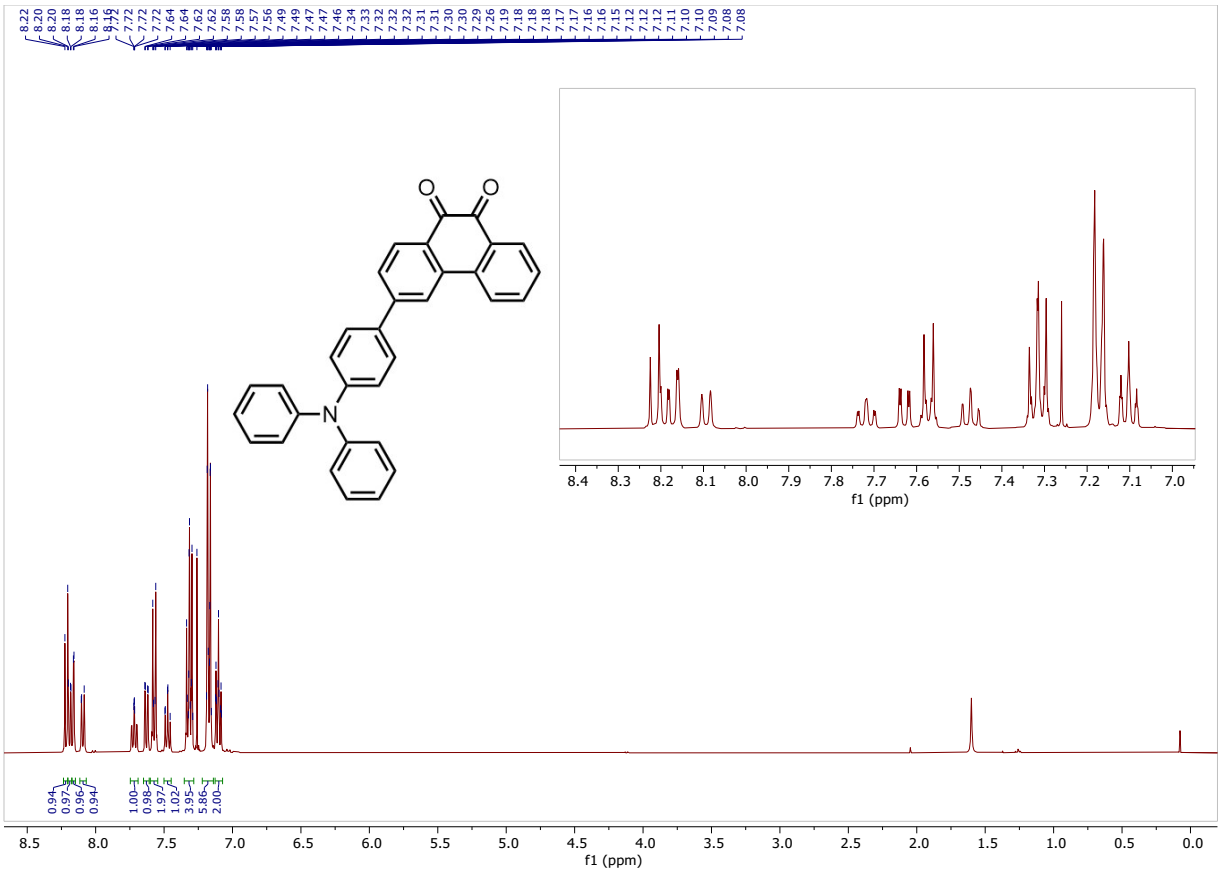

Figure S27: ^{1}H NMR spectrum of 3-(4-(diphenylamino)phenyl)phenanthrene-9,10-dione (**3-3**) in $CDCl_3$.

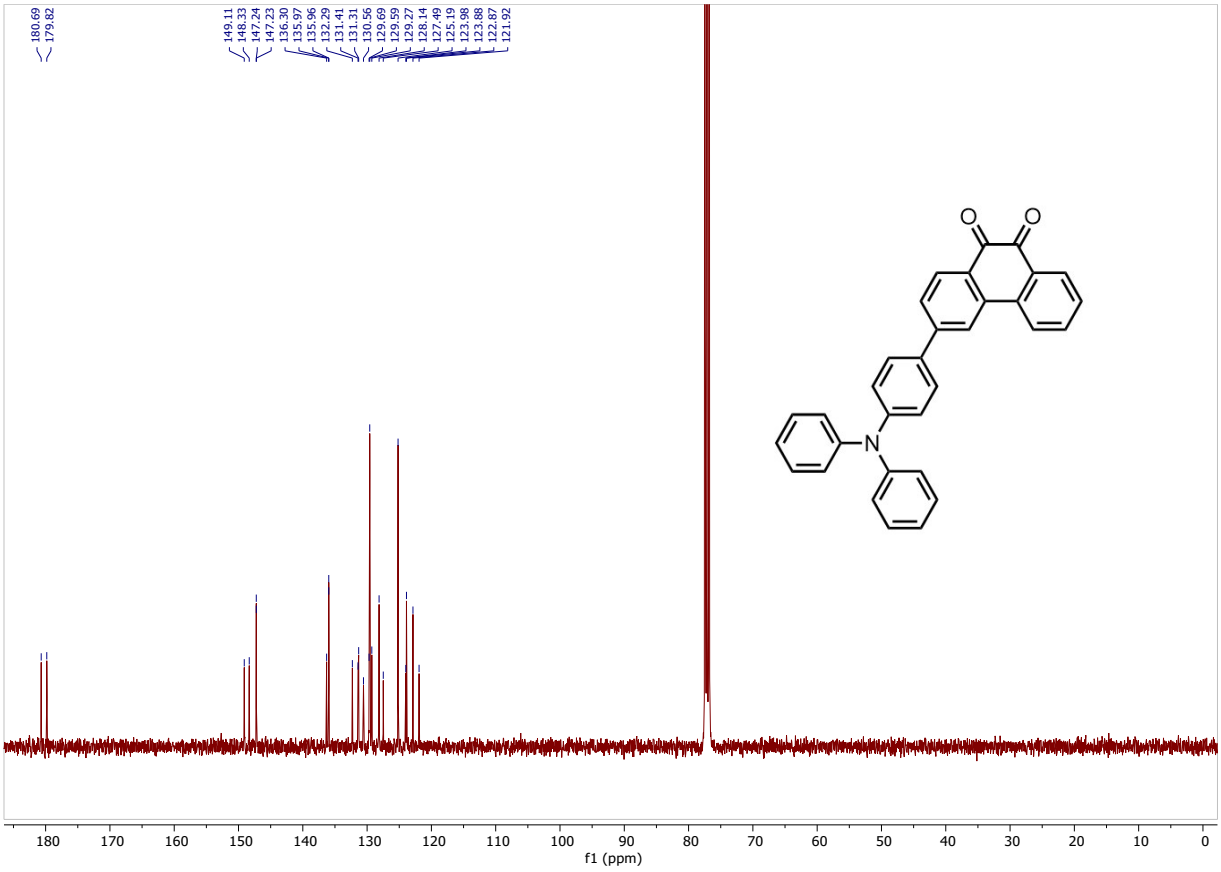

Figure S28: ^{13}C NMR spectrum of 3-(4-(diphenylamino)phenyl)phenanthrene-9,10-dione (**3-3**) in $CDCl_3$.

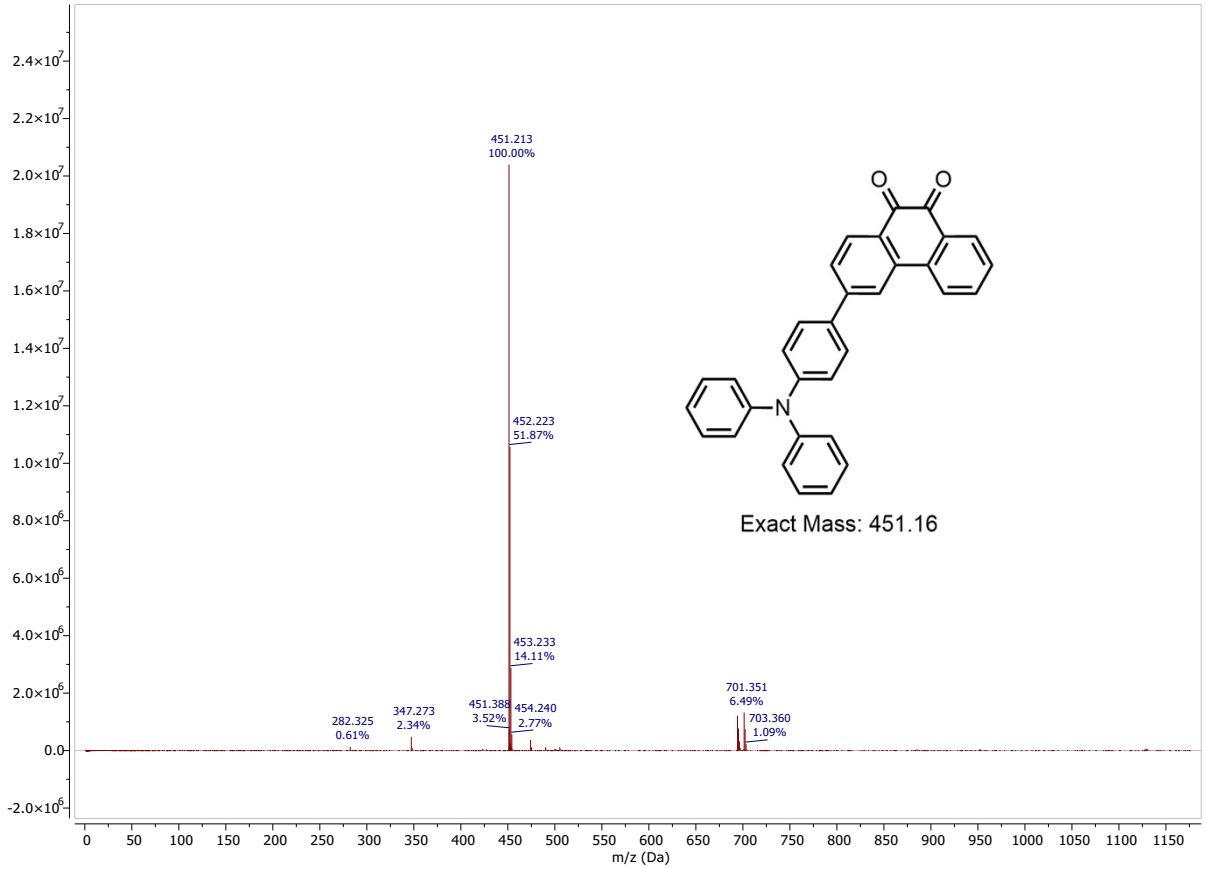

Figure S29: MALDI-ToF mass spectrum of 3-(4-(diphenylamino)phenyl)phenanthrene-9,10-dione (**3-3**).

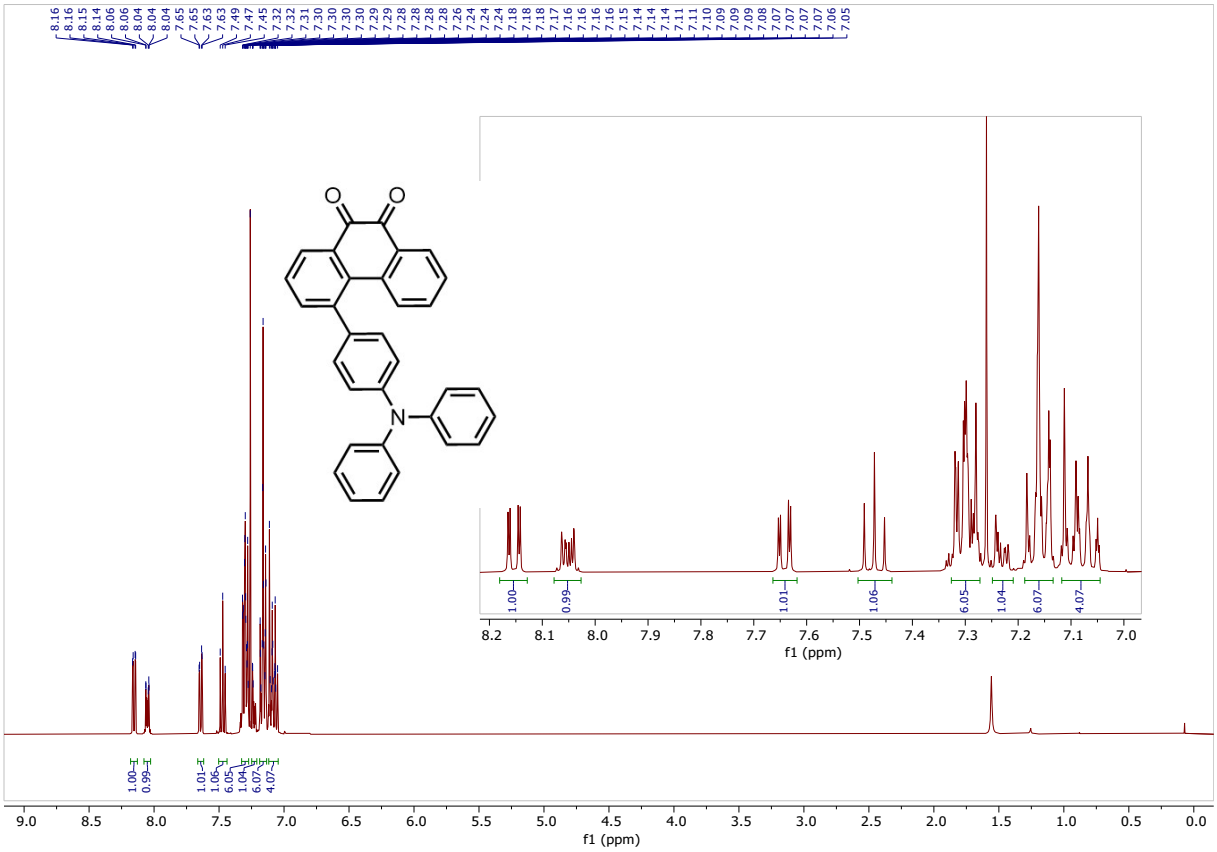

Figure S30: ^{1}H NMR spectrum of 4-(4-(diphenylamino)phenyl)phenanthrene-9,10-dione (**3-4**) in $CDCl_3$.

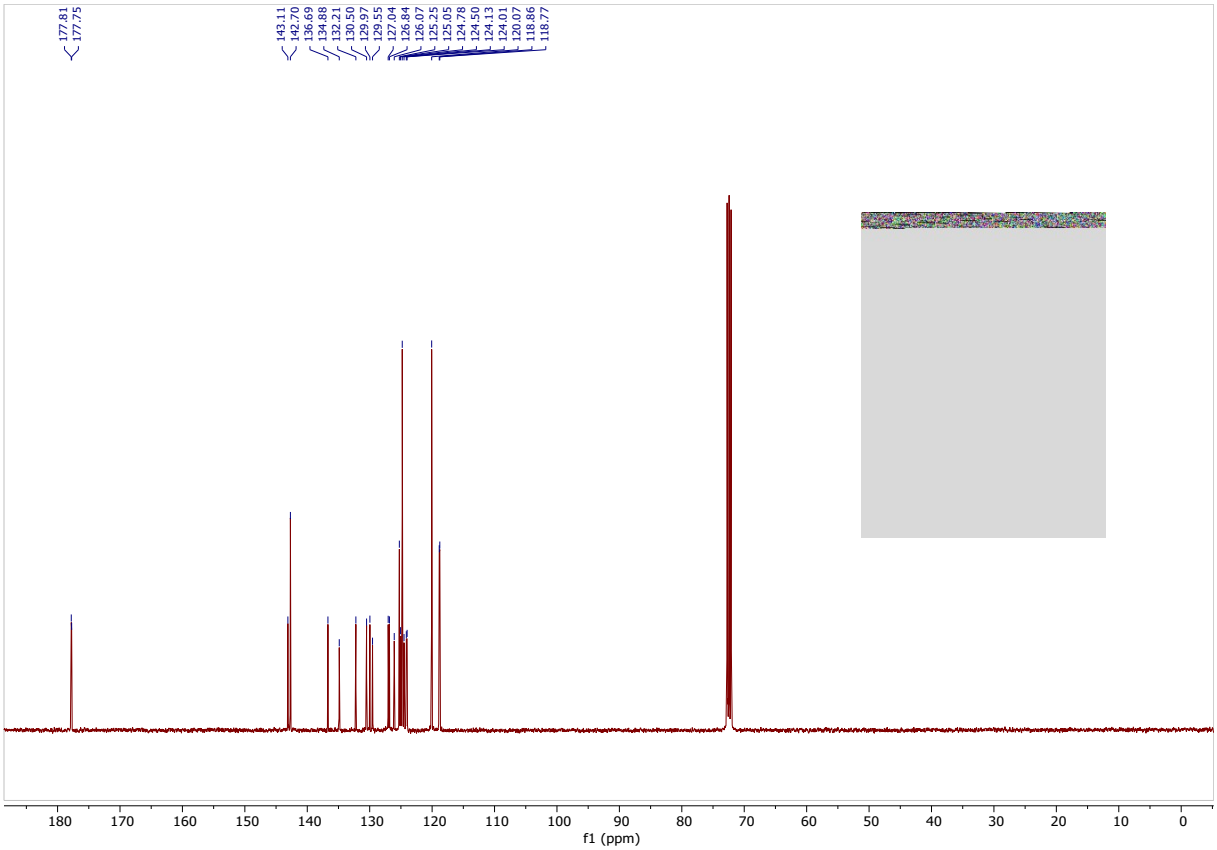

Figure S31: ^{13}C NMR spectrum of 4-(4-(diphenylamino)phenyl)phenanthrene-9,10-dione (**3-4**) in $CDCl_3$.

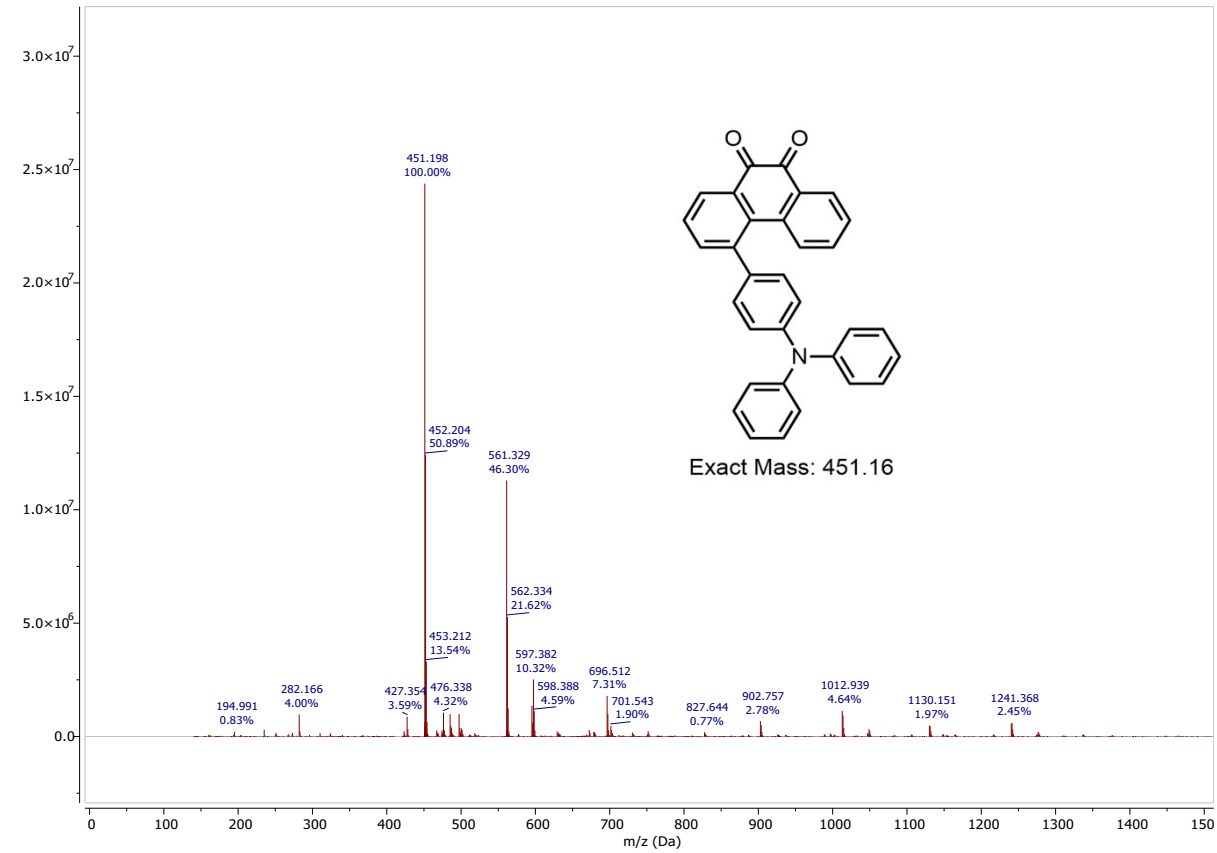

Figure S32: MALDI-ToF mass spectrum of 4-(4-(diphenylamino)phenyl)phenanthrene-9,10-dione (**3-4**).

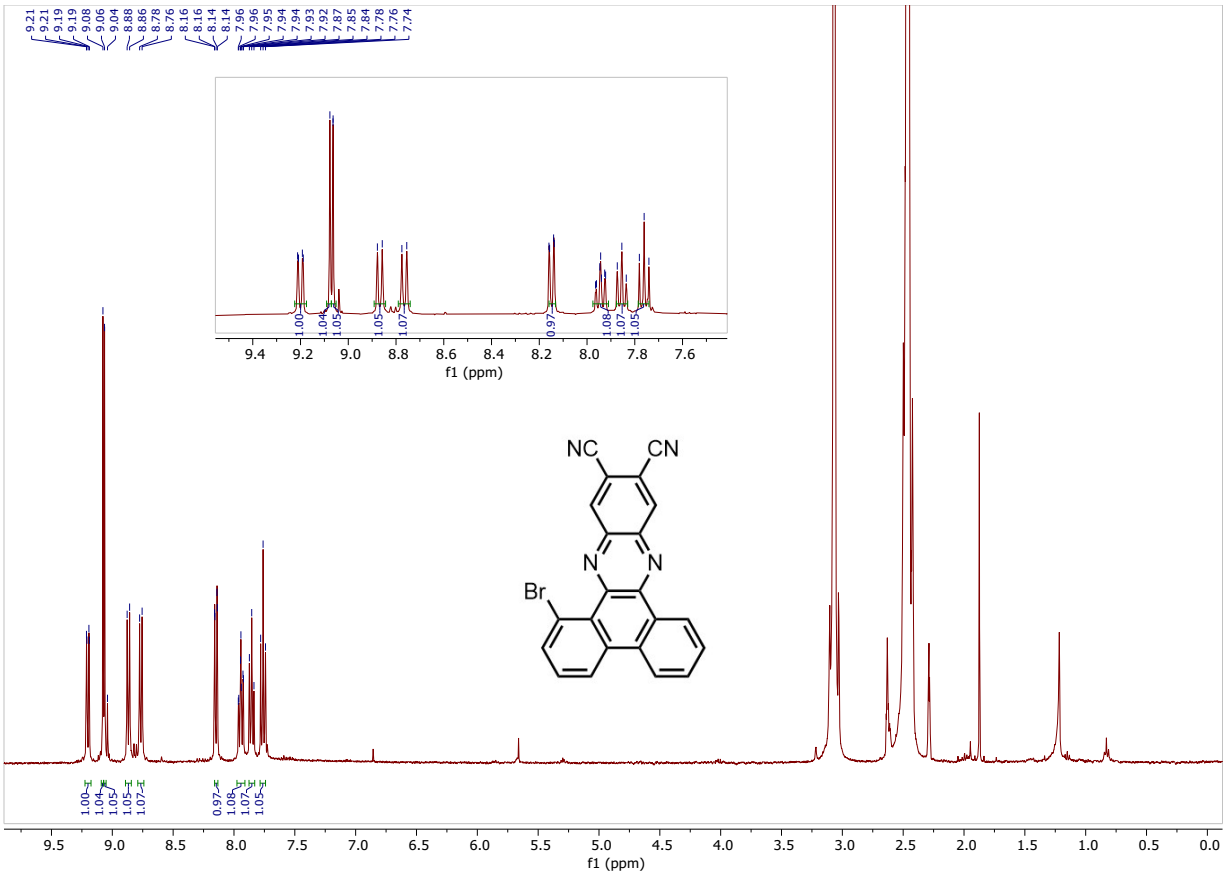

Figure S33: ^{1}H NMR spectrum of 1-bromodibenzo[*a*,*c*]phenazine-11,12-dicarbonitrile (**4-1**) in DMSO-d_6.

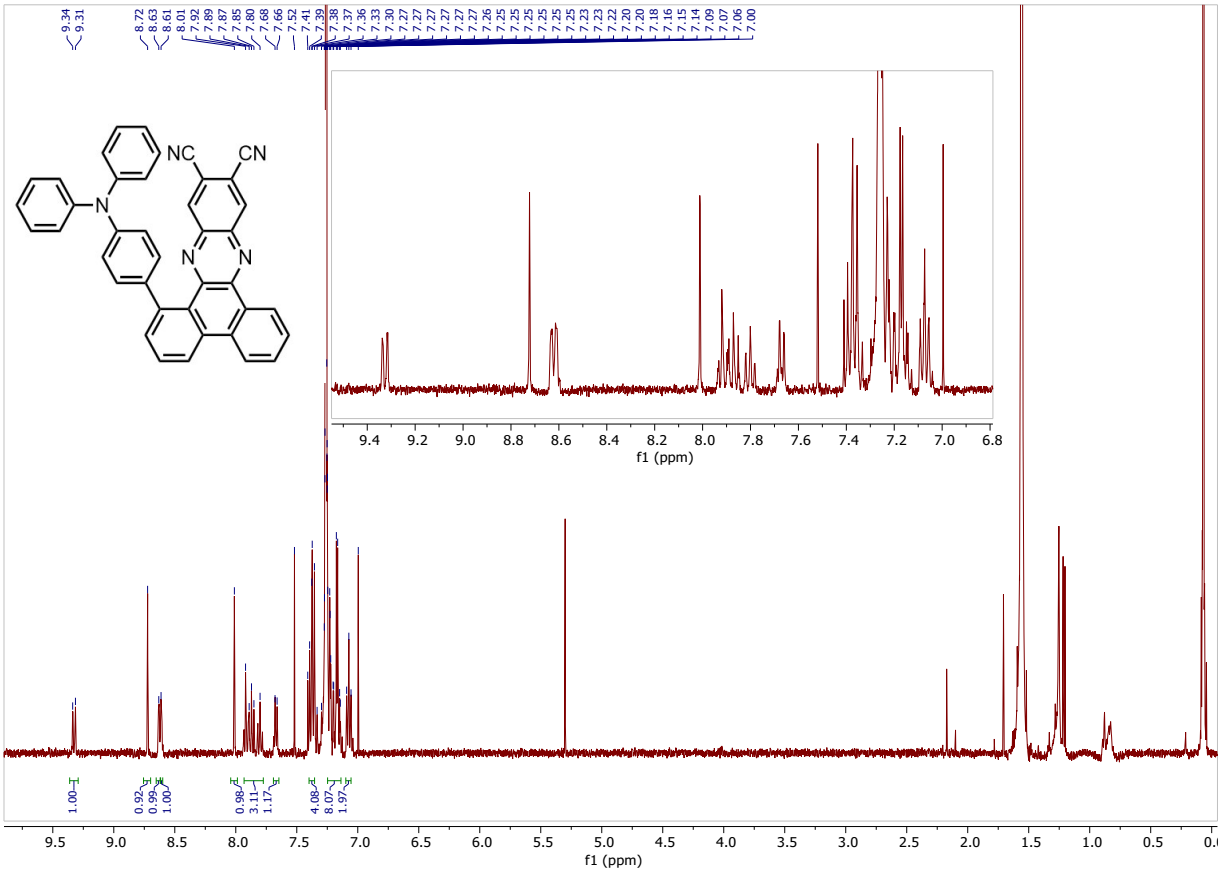

Figure S34: ^{1}H NMR spectrum of 1-(4-(diphenylamino)phenyl)dibenzo[*a*,*c*]phenazine-11,12-dicarbonitrile (**5-1**) in $CDCl_3$.

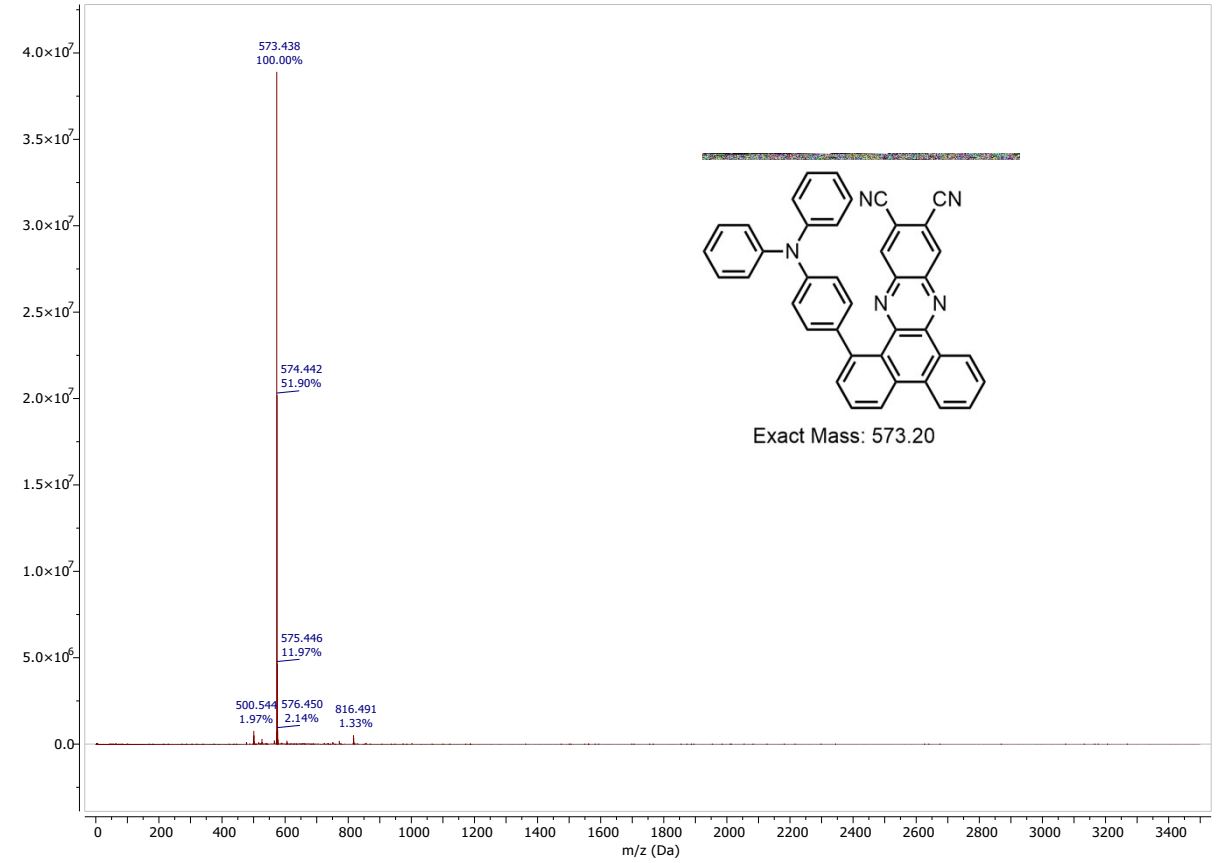

Figure S35: MALDI-ToF mass spectrum of 1-(4-(diphenylamino)phenyl)dibenzo[*a*,*c*]phenazine-11,12-dicarbonitrile (**5-1**).

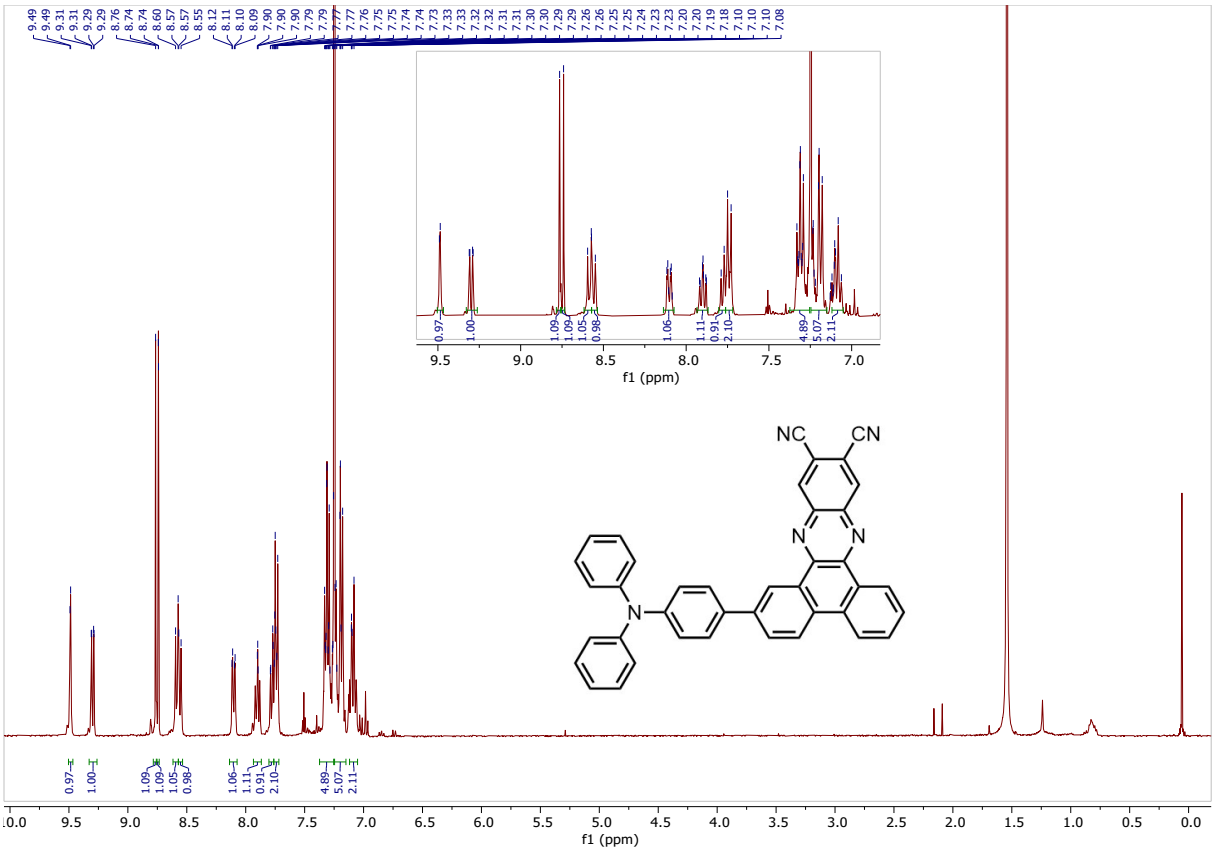

Figure S36: ^{1}H NMR spectrum of 2-(4-(diphenylamino)phenyl)dibenzo[*a*,*c*]phenazine-11,12-dicarbonitrile (**5-2**) in $CDCl_3$.

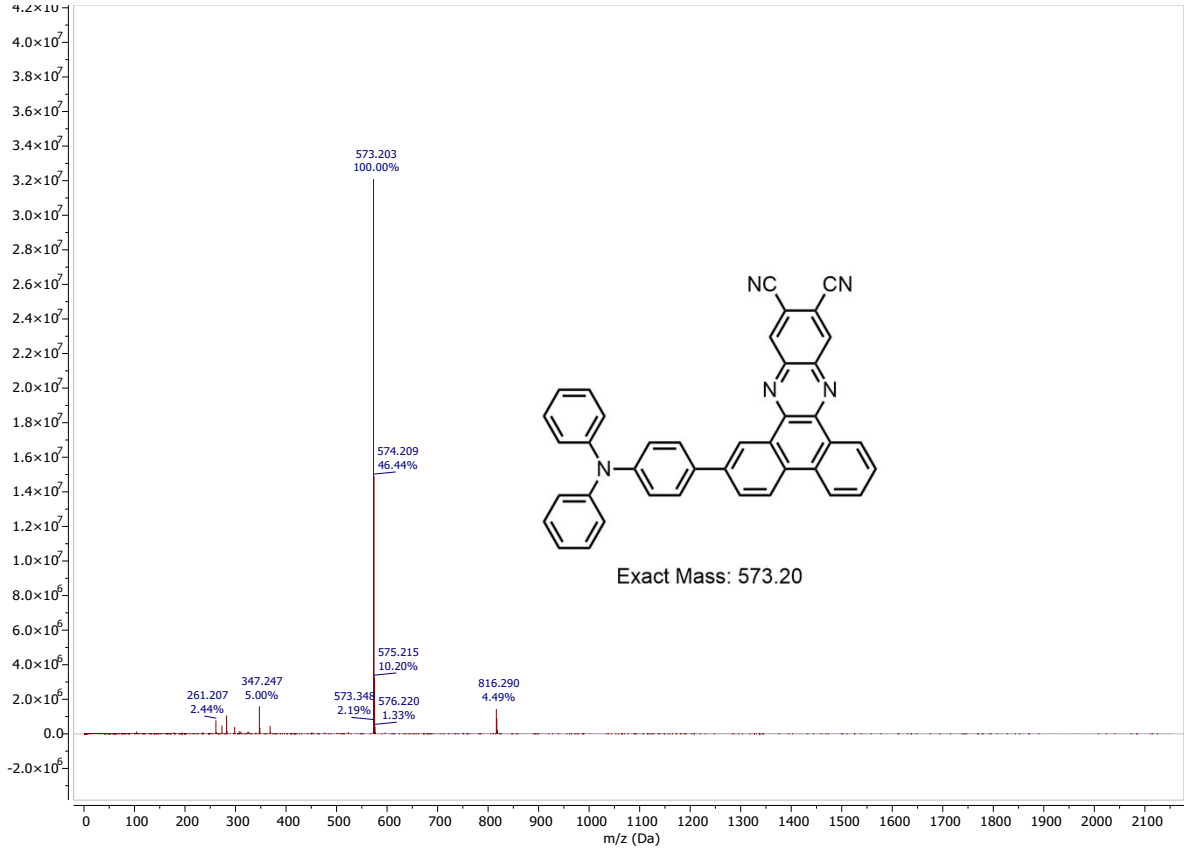

Figure S37: MALDI-ToF mass spectrum of 1-(4-(diphenylamino)phenyl)dibenzo[*a*,*c*]phenazine-11,12-dicarbonitrile (**5-2**).

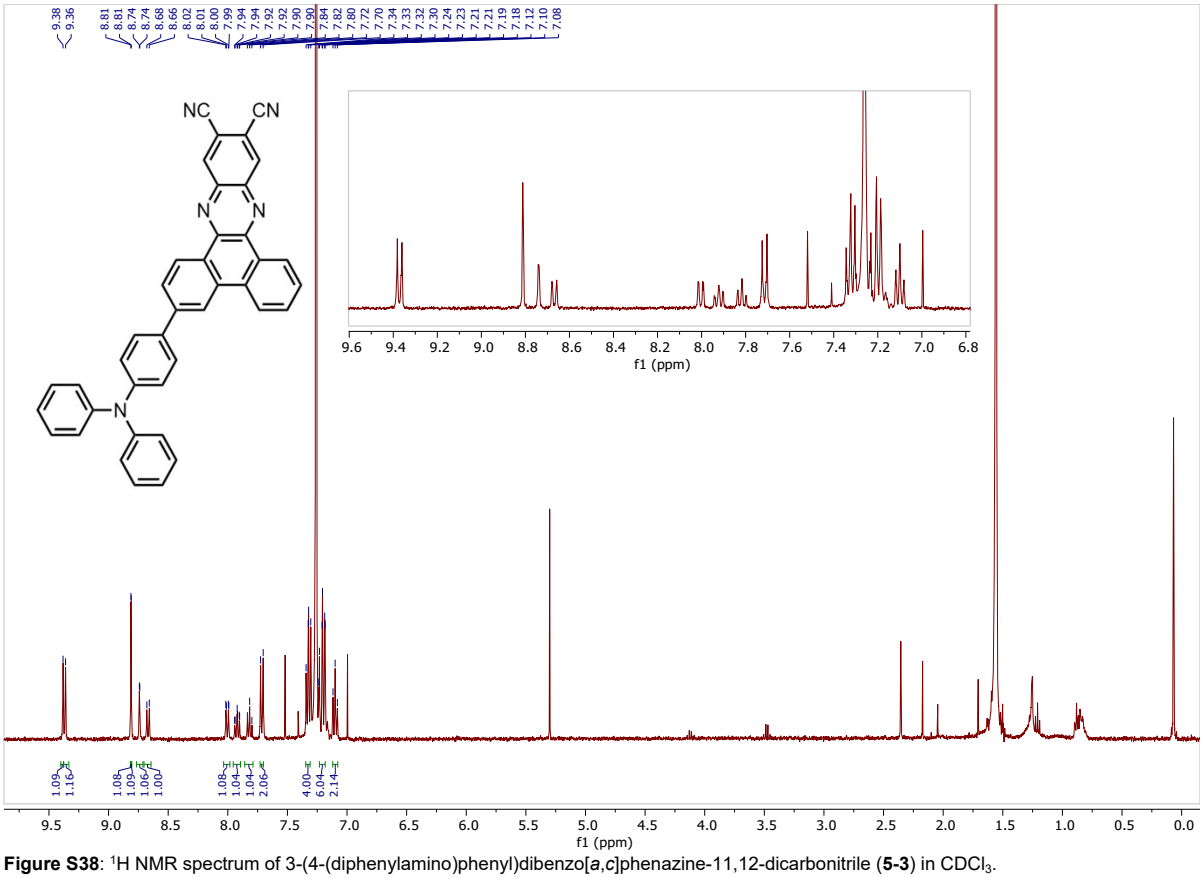

Figure S38: ^{1}H NMR spectrum of 3-(4-(diphenylamino)phenyl)dibenzo[*a*,*c*]phenazine-11,12-dicarbonitrile (**5-3**) in $CDCl_3$.

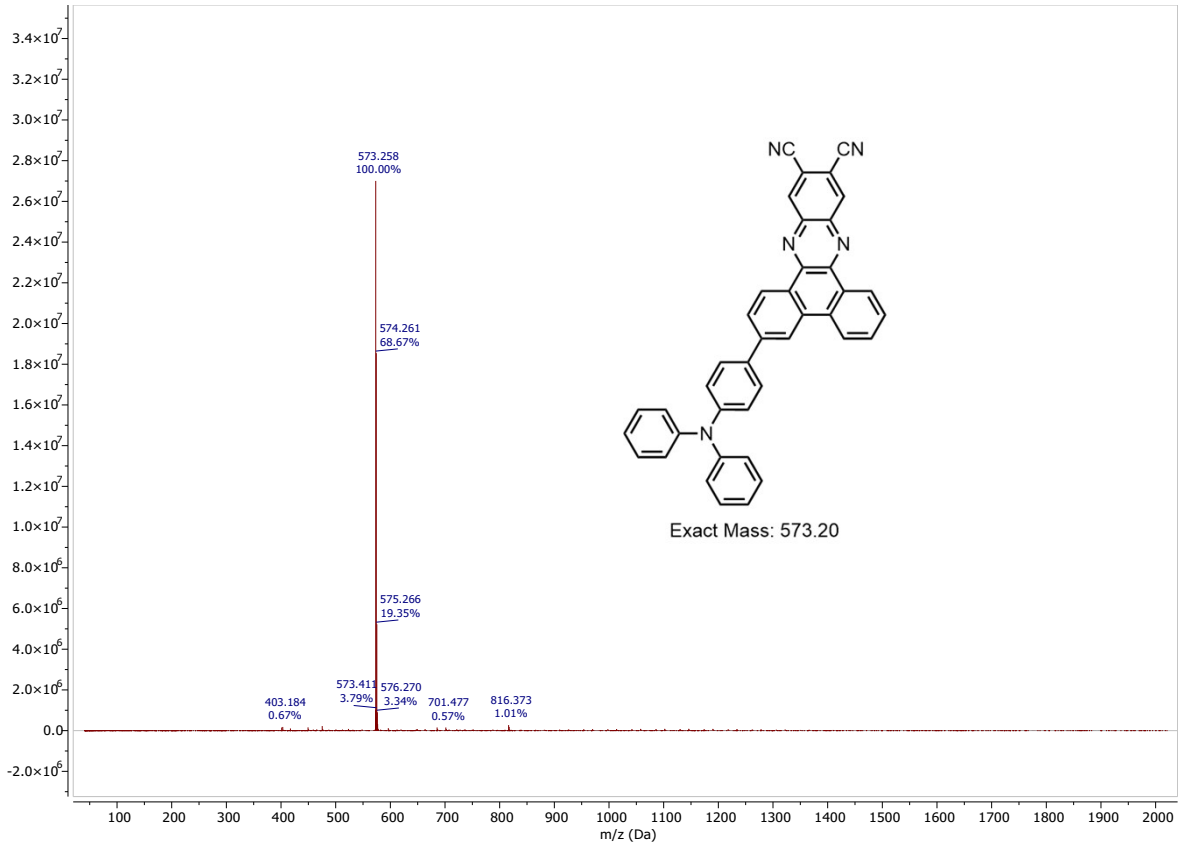

Figure S39: MALDI-ToF mass spectrum of 3-(4-(diphenylamino)phenyl)dibenzo[*a*,*c*]phenazine-11,12-dicarbonitrile (**5-3**).

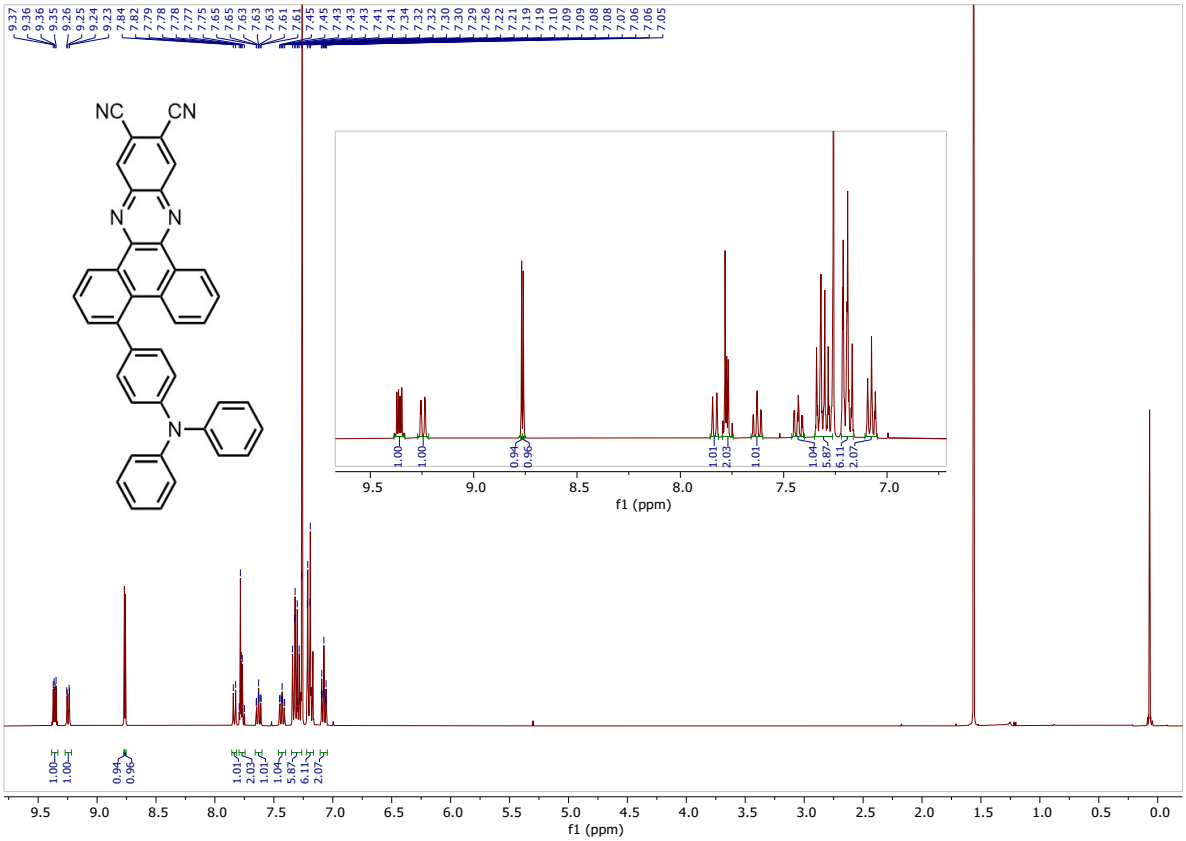

Figure S40: ^{1}H NMR spectrum of 4-(4-(diphenylamino)phenyl)dibenzo[*a*,*c*]phenazine-11,12-dicarbonitrile (**5-4**) in $CDCl_3$.

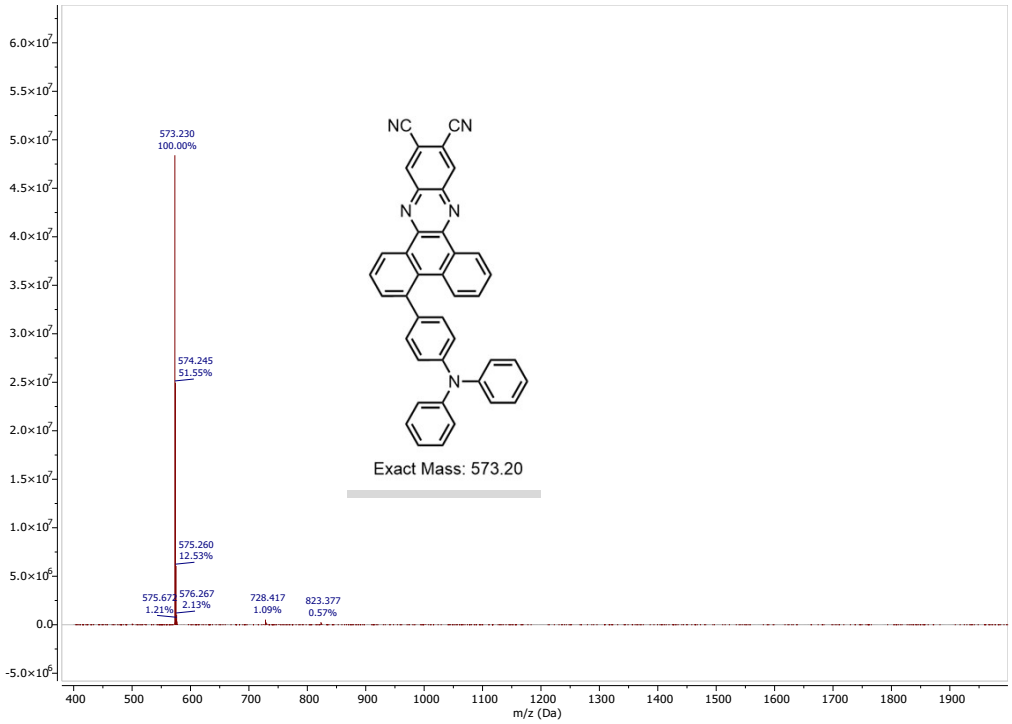

Figure S41: MALDI-ToF mass spectrum of 4-(4-(diphenylamino)phenyl)dibenzo[*a*,*c*]phenazine-11,12-dicarbonitrile (**5-4**).

15. Coordinates of optimized geometries

1-TPA-DBPzCN

C	-2.83855	-1.64502	-0.49114
C	-4.14377	-2.18802	-0.52246
C	-5.28842	-1.40330	-0.04206
C	-5.11156	-0.07765	0.39696
C	-3.80110	0.54184	0.30234
N	-3.66760	1.80984	0.63397
C	-2.46537	2.38566	0.45727
C	-2.26908	3.73775	0.81126
C	-1.05729	4.34192	0.58647
C	0.01650	3.60745	-0.01290
C	-0.15715	2.29066	-0.35479
C	-1.39392	1.65595	-0.11429
N	-1.53097	0.35972	-0.42496
C	-2.68361	-0.22548	-0.18852
C	-4.31401	-3.49245	-0.99939
C	-3.23627	-4.24848	-1.40519
C	-1.94800	-3.74121	-1.29135
C	-1.72542	-2.45808	-0.81789
C	-6.19509	0.65812	0.89079
C	-7.45174	0.10048	0.95625
C	-7.64042	-1.21004	0.52149
C	-6.57962	-1.94412	0.03314
C	-0.31475	-2.04873	-0.60565
C	0.18004	-1.89193	0.68815
C	1.49300	-1.52143	0.90958
C	2.35875	-1.31148	-0.16637
C	1.86983	-1.47825	-1.46230
C	0.55176	-1.85062	-1.67439
N	3.70420	-0.94616	0.05174
C	4.29531	0.02361	-0.80211
C	4.50123	-1.60941	1.00407
C	5.40234	-0.30285	-1.58097
C	5.97183	0.65043	-2.41155

C	5.43785	1.93093	-2.47814
C	4.33496	2.26051	-1.70057
C	3.76925	1.31155	-0.86212
C	5.54649	-0.93014	1.63554
C	6.34561	-1.57862	2.56255
C	6.11514	-2.90823	2.89023
C	5.07552	-3.58526	2.26728
C	4.27930	-2.95056	1.32724
C	-0.87204	5.70922	0.94623
N	-0.72765	6.81537	1.23939
C	1.27142	4.23647	-0.26078
N	2.29328	4.72888	-0.47109
H	-3.09526	4.28650	1.25502
H	0.64004	1.70462	-0.80983
H	-5.30517	-3.92870	-1.06292
H	-3.39336	-5.25535	-1.78406
H	-1.08985	-4.36010	-1.54531
H	-6.01667	1.67872	1.21588
H	-8.28804	0.67703	1.34273
H	-8.62766	-1.66321	0.56890
H	-6.76717	-2.96476	-0.28392
H	-0.48694	-2.04235	1.53638
H	1.86469	-1.39717	1.92448
H	2.53737	-1.32322	-2.30759
H	0.18172	-1.96910	-2.69173
H	5.81176	-1.30978	-1.52414
H	6.83616	0.38794	-3.01755
H	5.88662	2.67634	-3.13017
H	3.92552	3.26805	-1.72193
H	2.92843	1.56807	-0.21778
H	5.72594	0.11545	1.39524
H	7.15292	-1.03057	3.04361
H	6.74042	-3.41202	3.62299
H	4.88679	-4.63036	2.50393
H	3.47921	-3.49664	0.83285

2-TPA-DBPzCN

C	-0.85391	-1.04308	-0.05532
C	0.27041	-1.85382	-0.05547
C	0.06471	-3.24182	-0.04181
C	-1.20234	-3.77967	-0.02603
C	-2.34472	-2.96870	-0.02372
C	-2.14531	-1.57445	-0.04050
C	-3.69838	-3.52313	-0.00388
C	-4.81494	-2.66328	0.01337
C	-4.62438	-1.22105	0.00672
C	-3.29098	-0.67588	-0.02513
C	-3.93802	-4.90411	0.00083
C	-5.22071	-5.41046	0.02256
C	-6.31829	-4.55131	0.04102
C	-6.11146	-3.19035	0.03622
N	-5.68079	-0.43568	0.02883
N	-3.08707	0.62430	-0.03880
C	1.62641	-1.28323	-0.06175
C	-4.16355	1.42970	-0.01744
C	-5.47629	0.89295	0.01888
C	-3.98523	2.82954	-0.02948
C	-5.07117	3.66730	-0.00434
C	-6.39562	3.12587	0.03428
C	-6.58391	1.76724	0.04498
C	1.91639	-0.10796	-0.75983
C	3.18730	0.43352	-0.76413
C	4.22257	-0.17427	-0.04814
C	3.94178	-1.34813	0.65583
C	2.67124	-1.89178	0.63797
N	5.51128	0.38485	-0.03472

C	6.65419	-0.44929	0.02157
C	5.68282	1.79065	-0.02787
C	7.69430	-0.15706	0.90298
C	8.81825	-0.96655	0.94863
C	8.91474	-2.08380	0.12977
C	7.87745	-2.37952	-0.74518
C	6.75772	-1.56541	-0.80816
C	6.65367	2.38158	-0.83565
C	6.83495	3.75539	-0.81688
C	6.04339	4.55903	-0.00702
C	5.07223	3.97290	0.79401
C	4.89657	2.59822	0.79353
C	-7.52419	3.99708	0.06221
N	-8.44174	4.69552	0.08514
C	-4.87509	5.07961	-0.01582
N	-4.70798	6.22077	-0.02523
H	-0.75124	0.03865	-0.03798
H	0.92271	-3.91045	-0.07019
H	-1.29912	-4.86107	-0.02377
H	-3.10717	-5.60274	-0.01351
H	-5.37170	-6.48727	0.02517
H	-7.32857	-4.95156	0.05855
H	-6.94743	-2.49739	0.04966
H	-2.97290	3.22308	-0.05770
H	-7.58188	1.33866	0.07383
H	1.13699	0.37378	-1.34745
H	3.39087	1.33570	-1.33610
H	4.72858	-1.82671	1.23410
H	2.47686	-2.78870	1.22359
H	7.61380	0.71225	1.55223
H	9.62203	-0.72699	1.64117
H	9.79506	-2.72034	0.17168
H	7.94578	-3.24638	-1.39866
H	5.95213	-1.78844	-1.50462
H	7.26642	1.75281	-1.47834
H	7.59577	4.20299	-1.45238
H	6.18327	5.63708	0.00064
H	4.45204	4.59079	1.43952
H	4.14594	2.13902	1.43329

3-TPA-DBPzCN

C	-1.68180	-1.30564	-0.03762
C	-0.31054	-1.38492	-0.04737
C	0.47096	-0.21848	-0.04104
C	-0.18158	1.00847	-0.02262
C	-1.57384	1.11998	-0.01631
C	-2.33370	-0.06648	-0.02233
C	-2.24619	2.42290	0.00564
C	-3.65330	2.49252	0.01662
C	-4.44537	1.27128	0.00781
C	-3.78365	-0.00889	-0.01199
C	-1.53307	3.62883	0.01332
C	-2.18003	4.84683	0.03221
C	-3.57236	4.90494	0.04353
C	-4.29797	3.73491	0.03542
N	-5.75790	1.36024	0.01844
N	-4.47289	-1.13205	-0.01905
C	7.92605	-1.84575	0.89593
C	8.61081	-3.05038	0.92279
C	8.22555	-4.09723	0.09594
C	7.15148	-3.92496	-0.76745
C	6.47209	-2.71786	-0.81155
C	6.57449	1.82411	0.82667
C	7.31628	2.99467	0.81647
C	8.41612	3.12343	-0.02171
C	8.76454	2.07034	-0.85708

C	8.01774	0.90274	-0.86387
C	6.91644	0.77006	-0.01973
N	6.16438	-0.43104	-0.01415
C	6.85098	-1.66937	0.02605
C	-6.46522	0.21587	0.01071
C	-5.81432	-1.04465	-0.00806
C	-7.87474	0.27088	0.02189
C	-8.61479	-0.88464	0.01497
C	-7.95875	-2.15632	-0.00366
C	-6.58858	-2.22482	-0.01491
C	4.76218	-0.38987	-0.03098
C	4.00504	-1.34861	0.64878
C	2.62433	-1.29847	0.62840
C	1.93972	-0.28597	-0.04927
C	2.70617	0.66662	-0.72712
C	4.08602	0.61557	-0.72874
C	-8.72623	-3.35814	-0.01042
N	-9.33947	-4.33497	-0.01586
C	-10.03877	-0.81441	0.02660
N	-11.19038	-0.75047	0.03613
H	-2.28951	-2.20564	-0.05196
H	0.17311	-2.35819	-0.09006
H	0.43017	1.90436	0.02185
H	-0.44774	3.62298	0.00348
H	-1.59595	5.76393	0.03801
H	-4.08190	5.86481	0.05805
H	-5.38375	3.74952	0.04329
H	8.22118	-1.02834	1.55055
H	9.44778	-3.17472	1.60615
H	8.76108	-5.04290	0.12283
H	6.84664	-4.73455	-1.42673
H	5.64089	-2.57765	-1.49942
H	5.72231	1.71697	1.49451
H	7.04001	3.80906	1.48246
H	9.00036	4.04023	-0.02246
H	9.62137	2.16134	-1.52076
H	8.28378	0.08053	-1.52492
H	-8.35532	1.24529	0.03613
H	-6.07442	-3.18189	-0.02909
H	4.51078	-2.12996	1.21099
H	2.06443	-2.03993	1.19545
H	2.20978	1.44327	-1.30612
H	4.65572	1.35497	-1.28653

4-TPA-DBPzCN

C	1.45770	-1.18808	-0.91381
C	-2.51350	-2.47185	-1.78139
C	-1.42469	-3.20451	-2.19345
C	-0.14894	-2.72887	-1.91981
C	0.06286	-1.50233	-1.30088
C	-1.04773	-0.67603	-0.99559
C	-2.33791	-1.22633	-1.17203
C	-0.93458	0.72154	-0.54130
C	-2.05240	1.37454	0.02111
C	-3.35244	0.72536	0.02599
C	-3.50983	-0.53329	-0.65237
C	0.23163	1.48609	-0.70706
C	0.31430	2.78767	-0.25642
C	-0.76908	3.38777	0.38059
C	-1.94723	2.68685	0.49786
N	-4.37517	1.32797	0.59476
N	-4.69199	-1.10006	-0.76791
C	-5.58059	0.73945	0.50114
C	-5.74408	-0.48050	-0.20426
C	-6.70170	1.34966	1.10270
C	-7.94280	0.77407	1.00047

C	-8.10926	-0.45192	0.28099
C	-7.02732	-1.05846	-0.30524
C	2.47380	-1.11106	-1.86459
C	3.77146	-0.79662	-1.49829
C	4.08998	-0.55338	-0.16145
C	3.08261	-0.66634	0.79975
C	1.79124	-0.98558	0.42547
N	5.40196	-0.19458	0.20679
C	5.97664	-0.71746	1.38833
C	6.11994	0.73989	-0.57519
C	6.70780	0.10501	2.24563
C	7.27582	-0.41656	3.39710
C	7.11084	-1.75681	3.72047
C	6.37625	-2.57543	2.87276
C	5.81967	-2.06575	1.71069
C	7.47501	0.54383	-0.84192
C	8.17821	1.46739	-1.59866
C	7.54122	2.58871	-2.11389
C	6.19072	2.78256	-1.85574
C	5.48448	1.87225	-1.08573
C	-9.39952	-1.04912	0.17229
N	-10.43978	-1.53859	0.07980
C	-9.06689	1.40277	1.61239
N	-9.97153	1.91681	2.11004
H	-3.52489	-2.84527	-1.90756
H	-1.55823	-4.16755	-2.67912
H	0.71910	-3.34352	-2.15159
H	1.09139	1.06467	-1.21413
H	1.23535	3.34548	-0.40932
H	-0.69746	4.40749	0.74984
H	-2.82915	3.14288	0.93766
H	-6.55760	2.28179	1.64206
H	-7.13446	-1.99134	-0.85185
H	2.23695	-1.27644	-2.91473
H	4.55178	-0.72812	-2.25304
H	3.32031	-0.49206	1.84668
H	1.01298	-1.04955	1.18433
H	6.82803	1.15833	2.00164
H	7.84316	0.23727	4.05574
H	7.55261	-2.16123	4.62769
H	6.24544	-3.62886	3.11007
H	5.25736	-2.71222	1.04011
H	7.97268	-0.34024	-0.44916
H	9.23433	1.30066	-1.79844
H	8.09434	3.30768	-2.71296
H	5.68168	3.66082	-2.24667
H	4.42942	2.03370	-0.87155

16. References

1. A. M. Brouwer, Pure and Applied Chemistry, 2011, **83**, 2213-2228.
2. F. Wilkinson, W. P. Helman and A. B. Ross, Journal of Physical and Chemical Reference Data, 1993, **22**, 113-262.
3. S. Trasatti, Pure and Applied Chemistry, 1986, **58**, 955-966.
4. A. J. Bard, L. R. Faulkner and H. S. White, Electrochemical Methods: Fundamentals and Applications, 3rd Edition, 2022.
5. O. V. Dolomanov, L. J. Bourhis, R. J. Gildea, J. A. K. Howard and H. Puschmann, Journal of Applied Crystallography, 2009, **42**, 339-341.
6. G. Sheldrick, Acta Crystallographica Section A, 2008, **64**, 112-122.
7. A. Urbano, A. M. del Hoyo, A. Martínez-Carrión and M. C. Carreño, Organic Letters, 2019, **21**, 4623-4627.
8. T. Matsushima, S. Kobayashi and S. Watanabe, The Journal of Organic Chemistry, 2016, **81**, 7799-7806.
9. J. Kumsampao, C. Chaiwai, P. Chasing, T. Chawanpunyawat, S. Namuangruk, T. Sudyoadsuk and V. Promarak, Chemistry – An Asian Journal, 2020, **15**, 3029-3036.
10. A. m. Thangthong, N. Prachumrak, R. Tarsang, T. Keawin, S. Jungsuttiwong, T. Sudyoadsuk and V. Promarak, Journal of Materials Chemistry, 2012, **22**, 6869-6877.